Food and Energy Security

WILEY

Food and Energy Security Open Access

ORIGINAL ARTICLE OPEN ACCESS

Genome-Wide Association Study and RNA Sequencing Identify Candidate Genes Regulating Nitrogen Use Efficiency and Associated Traits in Sorghum (*Sorghum bicolor* (L.) Moench)

Srikanth Bollam[1] | Laavanya Rayaprolu[1,2] | Kirandeep Kaur Romana[1] | Pradeep Ruperao[1] | Sivasubramani Selvanayagam[1,2] | Anil Kumar Vemula[1] | Gopikrishna Adapala[1,3] | Vinod Kumar Valluri[1] | Prasad Bajaj[1] | Abhishek Rathore[1,3] | Damaris A. Odeny[1] | Rakesh K. Srivastava[1] | Santosh P. Deshpande[1] | Rajeev Gupta[1,4]

[1]International Crops Research Institute for the Semi-Arid Tropics, Hyderabad, India | [2]Wageningen University & Research, Wageningen, the Netherlands | [3]International Maize and Wheat Improvement Center (CIMMYT), Nairobi, Kenya | [4]US Department of Agriculture, Agricultural Research Service, Edward T. Schafer Agricultural Research Center, Fargo, North Dakota, USA

Correspondence: Rakesh K. Srivastava (rakesh.srivastava@icrisat.org) | Santosh P. Deshpande (ds1p2@yahoo.co.in) | Rajeev Gupta (rajeev.gupta@usda.gov)

Received: 21 April 2025 | **Revised:** 25 October 2025 | **Accepted:** 5 November 2025

Keywords: candidate gene | genome-wide association studies | genotypic variability | nitrogen use efficiency | sorghum | transcriptome analysis

ABSTRACT

Sorghum (*Sorghum bicolor* L. Moench) is a resilient cereal crop with remarkable adaptability to diverse environments. Nitrogen use efficiency (NUE) is critical for improving sorghum yields, resource utilization, livelihood security, and environmental sustainability of the target ecologies. To dissect the physio-genetic variation of sorghum for NUE/Nitrogen (N) stress tolerance, a set of 186 diverse sorghum accessions was evaluated for 15 agro-physiological and NUE-related traits under three N regimes (0%, 50%, and 100% of the recommended [90 kg ha^{-1}] dose) across two seasons. Genotyping-by-sequencing (GbS) SNP data enabled genome-wide association studies (GWAS). A total of 1369 marker-trait associations (MTAs) were detected across sorghum chromosomes, along with 69 candidate genes linked to N metabolism, including *glutamine synthetase* (*GS*), *nitrate transporters*, *and sucrose-phosphate synthase*. Transcriptome analysis of contrasting sorghum accessions detected 2229 (shoot) and 8661 (root) differentially expressed genes (DEGs). Integration of GWAS and transcriptomic data identified 10 key candidate genes such as the master N-regulators: the NIN-like protein (NLP), AP2/ERF transcription factor, ABC transporter, glutamine synthetase (GS), amino acid selective channel protein, F-box protein (FBP), SWEET transporter, glucose-1-phosphate adenylyltransferase (AGPase), and phosphofructokinase (PFK). Analysis of identified homologous gene groups across major cereals revealed evolutionary relationships and genetic conservation. Furthermore, this study identified contrasting sorghum accessions for N stress tolerance. The identified candidate genes and contrasting genetic stocks provide a foundation for the molecular dissection of NUE-related traits, offering clear targets for crop improvement via genomics-assisted breeding and gene editing technologies.

1 | Introduction

Sorghum (*Sorghum bicolor* L. Moench) is a highly popular and fifth most cultivated cereal crop after wheat (*Triticum aestivum* L.), rice (*Oryza sativa* L.), maize (*Zea mays* L.), and barley (*Hordeum vulgare*). It is widely distributed across North America, Africa, Asia, and Australia. It is a staple food crop for millions of poor people living in highly fragile agro-ecological zones of the semi-arid tropics

worldwide (Morris et al. 2013). Sorghum is a multipurpose crop, used as food, feed, fodder, forage, and alcoholic beverages (Silva et al. 2022). Additionally, sorghum has great economic potential as a source of fiber and feedstock for eco-friendly second-generation biofuels (Bollam et al. 2021).

The diploid nature (2n = 20), small genome size (812 Mb) of the cultivated sorghum and the variability in germplasm make it a model cereal for structural and functional genomic analysis. It is a C4 crop with good photosynthetic efficiency, deep root system architecture, and efficient use of nutrients, radiation, and water, which makes it adaptable to adverse and water-scant conditions (Paterson et al. 2008). Despite its C4 photosynthetic nature and relatively superior drought tolerance compared to maize (Paterson et al. 2009), sorghum continues to rely predominantly on nitrogen (N) fertilizer for achieving higher grain yields within intensive agricultural systems.

Over recent decades, the expansion of sorghum into both high-input and marginal environments has been accompanied by increasing attention to nitrogen use efficiency (NUE). While average N application rates remain lower than in maize, often $<100\,kg\,N\,ha^{-1}$ in different production ecologies (Wortmann 2006; Ciampitti and Prasad 2021), rising fertilizer costs and environmental pressures have heightened the need for accessions that maintain yields with reduced N inputs. Breeding for improved NUE could enable yield stability while cutting N fertilizer use by 20%–30% in some systems (Masclaux-Daubresse et al. 2010).

Nitrogen is the most important macronutrient for plant growth and one of the main factors contributing to high yield. N is the primary constituent of key biomolecules, including nucleotides, amino acids, proteins, and hormones. About 1.5%–2.0% of total plant dry matter and 16% of the plant protein were covered by N (Frink et al. 1999). On a global scale, N fertilizer is a widely used nutrient input, and it has contributed immensely to the productivity improvement of food crops. However, the production of nitrogen-based fertilizers consumes ~1% of the world's annual energy supply and increases food production expenditures (Erisman et al. 2008). Though N fertilizer is very expensive, it is considerably subsidized in the developing world for agricultural purposes, often leading to its excessive application. Nevertheless, plants can harness only 30%–40% of the applied N for their growth and development, while the remainder of the N fertilizer is lost to the environment through processes such as ammonia volatilization, denitrification, surface runoff, and leaching (Russo et al. 2017). This not only results in economic loss for the farmers but also exerts deleterious effects on neighbouring aquatic, plant, and animal ecosystems (Hirel, Chardon, and Durand 2007; Hirel, Le Gouis, et al. 2007; Srikanth et al. 2016).

To mitigate these impacts, it is crucial to adopt improved agronomic practices aimed at reducing fertilizer inputs, and employing nitrogen-efficient crop varieties is essential (Raun and Johnson 1999). NUE encompasses two key components: N uptake efficiency (NUpE), which measures the plant's ability to absorb and utilize available nitrogen from the soil, and N utilization efficiency (NUtE), which reflects the efficiency with which the absorbed nitrogen is assimilated and redistributed within the plant, ultimately contributing to grain production (Good et al. 2004). The basic definition of plant NUE is the grain yield achieved per unit of supplied nitrogen, a value that can also be expressed as the product of NUpE and NUtE (Good et al. 2004). Though efficient fertilizer management and modified N sources reduced the N losses to some extent, it's crucial to understand how crop plants respond to varied N availability scenarios and the genetic regulation of NUE remains essential (Raun and Johnson 1999).

NUE is a multifaceted phenomenon influenced by various genetic and environmental factors. Deciphering the genetic basis of such complex traits requires linking physiological and agronomic traits to molecular mechanisms (Hirel, Chardon, and Durand 2007). Gaining valuable insights in this context can open new avenues for selecting and breeding N-use efficient lines that can translate applied N into economically sustainable yields while minimizing environmental impact. Given the above background, the present study was undertaken with the following objectives: (1) to study the physiological responses of diverse sorghum accessions under varying N levels (2) to identify genes associated with NUE via a genome-wide association study (GWAS) (3) to investigate the global transcriptome profiles of contrasting sorghum accessions for NUE under different N conditions (4) integrated analysis of GWAS and global transcriptome analysis data to identify common genes, coupled with a comprehensive analysis of homologous gene groups across major cereals, to elucidate evolutionary relationships and genetic conservation. Our results provide novel insights pertaining to nitrogen uptake, assimilation, and remobilization, and elucidate mechanisms involved in N stress tolerance in sorghum.

2 | Results

2.1 | Genotypic and Nitrogen Regime Effects on Sorghum Morpho-Physiological and Yield-Related Traits

2.1.1 | Leaf Parameters

An increase in chlorophyll content (CC) was observed across N regimes, from N0 to N100 in both individual and pooled seasons (Tables 1 and 2). Leaf area (LA) was lowest under N50 compared to N0 and gradually increased further at N100. For both CC and LA, a significant genotype × treatment interaction for both individual and pooled seasons was observed along with notable season × genotype and season × genotype × treatment interactions. A decrease in leaf number (LN) from N0 to N50 treatments was followed by an increase at N100 in the year 2018 and across seasons with significant genotype × treatment interactions. In 2017–18, the genotype × treatment interaction for LN was significant at $p \leq 0.05$. For all leaf parameters, the season × genotype and season × genotype× treatment interactions were significant (Tables 1 and 2).

2.1.2 | Growth Parameters

Days to 50% flowering (DFL) showed minimal variability across seasons and N regimes, with significant genotype × treatment interactions in 2017–18 and pooled seasons with significance at

TABLE 1 | Performance of sorghum accessions under varied N regimes (0 N, 50% N, and 100% of the recommended N) for the seasons 2017–18, 2018–19, and across seasons.

		2017–18		2018–19		Across seasons	
Trait	**Treatment**	**Range**	**Mean**	**Range**	**Mean**	**Range**	**Mean**
Chlorophyll content	N0	20.01–47.67	34.30	31.60–51.55	43.08	26.79–47.29	38.69
	N50	23.18–53.86	38.48	37.34–55.58	46.90	34.15–53.91	42.67
	N100	30.82–63.33	43.88	37.37–54.49	46.30	37.33–54.63	45.10
Days to 50% flowering	N0	60–100	79.00	66.48–83.56	73.38	64.34–91.01	76.06
	N50	62–99	80.00	66.26–84.47	73.80	66.44–91.67	76.61
	N100	62–100	80.00	66.33–82.45	73.26	64.15–89.74	76.39
Leaf area (cm^2)	N0	389.43–4717.51	1704.98	659.89–9793.07	2693.76	599.58–6435.47	2203.43
	N50	394.20–4687.73	1886.08	637.99–8574.55	2345.91	605.53–5304.28	2119.29
	N100	433.14–6802.64	2334.35	699.00–10328.00	2726.04	610.28–6594.34	2515.72
Leaf number	N0	5.29–23.27	11.70	6.53–51.38	16.89	5.93–30.86	14.07
	N50	5.84–20.48	11.15	6.42–61.07	14.90	6.56–31.82	12.91
	N100	6.03–24.62	12.66	7.60–55.60	15.77	7.51–34.33	14.02
Plant height (cm)	N0	93.12–361.36	212.18	111.69–323.52	229.07	102.45–326.55	220.87
	N50	96.66–352.09	226.15	110.53–316.52	226.01	103.67–323.27	226.45
	N100	99.33–358.22	237.46	110.79–316.91	227.68	105.01–337.68	232.90
Number of tillers	N0	10.64–67.76	35.60	2.54–75.59	26.21	8.49–71.23	30.53
	N50	12.14–63.04	39.51	0.93–74.19	24.36	7.15–63.10	31.41
	N100	16.67–76.90	43.43	4.97–68.37	29.69	10.68–68.66	36.06
Number of panicles	N0	13.05–96.16	38.50	11.75–97.88	43.84	18.28–81.47	40.80
	N50	15.10–94.49	45.19	8.60–129.66	46.67	15.47–99.28	45.58
	N100	10.80–117.49	48.81	6.93–106.44	50.62	15.32–91.98	49.21
Panicle weight (g)	N0	150.24–1450.88	477.63	470.00–2622.55	1551.45	359.87–1676.73	1016.40
	N50	194.34–1932.85	590.78	554.66–2592.43	1641.18	386.88–2050.32	1118.27
	N100	212.97–1765.35	636.28	465.47–2602.24	1628.86	413.35–2069.98	1133.46
Panicle harvest index	N0	0.04–0.92	0.40	0.41–0.88	0.70	0.27–0.84	0.55
	N50	0.03–0.87	0.39	0.36–0.83	0.70	0.28–0.84	0.55
	N100	0.04–0.89	0.37	0.27–0.83	0.69	0.15–0.83	0.53
Grain yield (g)	N0	11.29–1031.31	242.69	210.27–1954.36	1087.29	125.92–1292.32	665.08
	N50	15.15–1402.00	305.00	293.78–1978.19	1161.51	181.73–1554.14	733.41
	N100	18.43–1294.15	316.73	192.42–1944.44	1139.57	135.74–1513.24	727.10
Test weight (g)	N0	0.12–4.89	1.88	1.74–5.29	2.74	1.17–4.30	2.31
	N50	0.27–4.73	1.96	1.59–5.26	2.70	1.02–4.75	2.33
	N100	0.56–4.34	1.83	1.68–4.99	2.72	1.25–4.29	2.28
Fresh straw yield (kg)	N0	1.72–9.63	4.64	1.75–7.50	4.43	2.63–7.41	4.54
	N50	1.81–10.89	5.61	2.45–9.41	4.87	3.51–7.66	5.25
	N100	1.63–12.99	5.97	2.86–8.51	5.00	3.05–9.31	5.48

(Continues)

TABLE 1 | (Continued)

Trait	Treatment	2017–18		2018–19		Across seasons	
		Range	Mean	Range	Mean	Range	Mean
Dry straw yield (kg)	N0	0.99–6.14	2.46	0.66–4.76	1.90	1.10–4.72	2.18
	N50	0.90–6.02	2.91	0.66–5.18	2.10	1.27–5.60	2.51
	N100	1.18–8.19	3.05	0.61–5.88	2.20	0.91–7.03	2.63
Harvest index	N0	10.43	0.07–74.31	40.84–88.02	69.69	22.07–73.79	40.09
	N50	11.69	0.04–73.23	36.33–83.28	70.06	18.84–71.27	40.93
	N100	11.14	0.24–74.21	26.81–82.86	68.70	14.25–77.13	40.02
N content in grain	N0	0.89–2.64	1.46	1.14–2.07	1.52	1.08–2.05	1.49
	N50	0.73–2.28	1.40	1.25–2.13	1.68	1.17–1.95	1.54
	N100	0.86–2.54	1.49	1.24–2.29	1.73	1.26–2.16	1.61
N content in straw	N0	0.12–1.00	0.37	0.18–0.69	0.35	0.16–0.65	0.36
	N50	0.12–0.899	0.35	0.16–0.78	0.39	0.18–0.74	0.37
	N100	0.18–1.11	0.44	0.17–0.87	0.40	0.22–0.77	0.42

Note: Data shown as the mean of three replications.

$p \leq 0.05$. A gradual increase in plant height (PH) was observed with increased N levels, with significant genotype × treatment, season × genotype, and season × genotype× treatment interactions. The number of tillers (NT) increased with a higher N in 2017–18 and pooled seasons, with significant genotype × treatment interactions in 2018–19 and pooled seasons, and significant season×genotype×treatment interactions ($p \leq 0.05$) (Tables 1 and 2).

2.1.3 | Panicle Parameters

The number of panicles (PN) increased with higher N dosage in both individual and pooled seasons, with significant season × genotype interactions ($p \leq 0.05$). Accordingly, in both individual and across seasons, the panicle weight (PW) also increased with higher N dosages, with significant genotype × treatment, season × genotype, and season × genotype× treatment interactions. Panicle harvest index (PHI) remained consistent in all three treatments, yet exhibited significant genotype × treatment, season × genotype, and season × genotype× treatment interactions in individual and pooled seasons (Tables 1 and 2).

2.1.4 | Biological Yield Parameters

Grain yield (GY) was slightly higher at N50 compared to N0 and N100, with a 9% increase in 2018–19 and a 6% increase across seasons. Test weight (TW) exhibited minimal variation across N regimes, except in 2017 where N50 recorded the highest seed weight. Both GY and TW displayed significant genotype × treatment, season × genotype, and season×genotype×treatment interactions. Fresh straw yield (FSY) and dry straw yield (DSY) increased with higher N dosages, with significant genotype × treatment, season × genotype, and season × genotype×treatment interactions (Tables 1 and 2). Harvest index (HI) varied across N regimes with significant treatment × genotype interactions in 2018 and across seasons and at ($p \leq 0.05$) in 2017–18.

2.1.5 | Grain and Stover N Content Parameters

Grain N content (GN) showed a quick plunge from N0 to N50, with a slight increment at N100 across seasons. Significant genotype× treatment and season× genotype interactions were observed. Straw N content (SN) also increased with the increase of N dosage and exhibited significant genotype × treatment, season × genotype, and season × genotype × treatment interactions (Tables 1 and 2).

2.2 | Correlation Coefficient Analysis of NUE and Agronomic Traits Under Varied N Regimes

Correlation coefficient analysis was conducted under three N regimes to evaluate the relationships among traits associated with NUE. Leaf area (LA) and leaf number (LN) were positively correlated with days to 50% flowering (DFL) under all N treatments and across seasons. Leaf number was also significantly correlated with LA in all treatments and seasons, and with the number of tillers (NT) under all treatments in 2017–18, and in N50 and N100 levels across seasons. Plant height (PH) showed a positive correlation with NT at N50 and N100 dosages in 2017–18 and across seasons and at N0 in 2018–19. Grain yield (GY) showed significant positive correlations with panicle weight (PW) and panicle harvest index (PHI) across all treatments and seasons, and with panicle number (PN) at N0 and N100 in both individual and across seasons. Dry stover yield (DSY) was positively correlated with PH under all treatments and with LA (except N0 in 2018–19). However, DSY exhibited negative correlations with GY and PW in 2017–18 and across seasons for all treatments. Overall, dry biomass was relatively negatively associated with PHI. Under all treatments, harvest

TABLE 2 | ANOVA summary for different traits under three N regimes in field trials during 2016–17, 2017–18, and across seasons.

		2017–18		2018–19		Across seasons						
S. No.	**Trait**	**Genotype (G)**	**G × T**	**Genotype (G)**	**G × T**	**Genotype (G)**	**Treatment (T)**	**Season (S)**	**G × T**	**S × G**	**S × T**	**S × G × T**
1	Chlorophyll content	24.36	13.53	4.3	2.72	11.47	62.37	39.70^{ns}	6.21	9.12	19.53^{ns}	6.47
2	Leaf area (cm^2)	17.36	6.41	17.1	5.5	23.02	24.32	51.00^{ns}	5.88	12.35	14.94^{ns}	6.04
3	Leaf number	2.5	1.19^{ns}	4.8	2.36	5.11	0.52^{ns}	3.35^{ns}	2.01	2.9	0.36^{ns}	1.85
4	Days to 50% flowering	52.06	2.22	11.81	1.29^{ns}	49.25	1.17^{ns}	393.87	1.97	27.14	0.72^{ns}	2.05
5	Plant height (cm)	170.76	8.07	132.36	4.29	256.3	168.41	5.3^{ns}	6.58	19.08	215.91	6.14
6	Number of tillers	8.04	0.96^{ns}	9.38	1.45	14.34	2.00^{ns}	6.34^{ns}	1.37	3.33	0.51^{ns}	1.3^{ns}
7	Number of panicles	8.69	1.07^{ns}	7.96	1.08^{ns}	13.57	21.34^{ns}	10.28^{ns}	1.14^{ns}	3.01^{ns}	1.57^{ns}	1.05^{ns}
8	Weight of panicles (g)	47.03	3.74	10.39	1.72	20.7	3.03^{ns}	601.63	2.14	11.65	0.35^{ns}	2.09
9	Panicle harvest index	60.47	2.84	5.32	1.5	45.44	4.93^{ns}	4022.04	2.33	31.58	1.05^{ns}	2.47
10	Grain yield (g)	72.51	3.30	11.54	2.24	28.43	2.27^{ns}	841.36	2.48	15.33	0.13^{ns}	2.44
11	Test weight (g)	41.61	5.47	3.36	2.02	13.46	2.01^{ns}	1558.04	2.99	8.8	4.95^{ns}	2.84
12	Fresh straw yield (kg)	38.37	4.57	1.72	1.98	9.88	34.12	19.49^{ns}	2.82	11.78	5.52^{ns}	2.81
13	Dry straw yield (kg)	25.48	3.17	15.34	1.46	30.54	25.05^{ns}	50.97^{ns}	2.73	10.21	3.04^{ns}	2.43
14	Harvest index	40.76	1.38^{ns}	5.21	1.50	26.73	3.40^{ns}	5992.90^{ns}	1.41	15.12	2.12	1.46
15	N content grain	9.31	1.28^{ns}	9.31	1.28^{ns}	12.63	7.09^{ns}	7.15^{ns}	1.30^{ns}	7.17	5.69^{ns}	1.23^{ns}
16	N content straw	10.45	4.71	10.45	4.71	7.32	47.11	0.88^{ns}	3.78	5.52	19.12^{ns}	3.54

Note: ns, not significant. All Fstat/genetic variance are significant @*p* of 0.001 except for traits with "ns."

index (HI) was positively correlated with GY and PW, whereas with PN at N0 in 2017–18 and N0 and N50 across seasons. Test weight (TW) was positively correlated with GY and PW across all treatments in 2017–18 and pooled seasons. Grain N content (GN) was negatively correlated with GY under N0 in individual and pooled seasons, and similar trends were observed for N50 and N100 in 2018–19 and pooled seasons. PW was also negatively correlated to GN at N0 in 2017–18 and across all treatments in 2018–19 and pooled seasons. DSY showed positive correlations with GN at N0 in individual and pooled seasons; at N50 in 2018–19 and across seasons ($p \leq 0.05$); and at N100 in 2018–19 ($p \leq 0.05$) and pooled seasons. Overall, GN and HI showed a negative correlation with each other. SN exhibited negative correlations with HI at N0 and N50 in individual and across seasons, and at N100 in 2017–18 and pooled seasons. Additionally, SN was negatively correlated with DSY across all treatments (Table 3).

2.3 | Population Structure and Diversity Analysis

The hierarchical population structure analysis assigned the 186 sorghum genotypes of the study into 5 subpopulations ($K = 5$) with some admixture in all the subpopulations using 22,439 SNPs (Figure 1a). The composition of possible groups, with different accessions contributing to each subpopulation, was represented by different colours (Figure 1a). Phylogenetic analysis using the GBS data also formed five distinctive clusters, thus supporting the findings of the structure analysis (Figure 1b).

2.4 | Identification of Contrasting Lines Under Low N Conditions

Based on the pooled grain yield data of 186 accessions evaluated under low N conditions, both high and low NUE lines were identified. High-NUE lines included IS15443, ICSV745, SSM1267, IS14276, IS2814, IS23903, IS2179, SI-3, IS30405, IS20700, IS27599, IS10234, IS4285, IS27791, IS20710, IS25596, 02.SB-FJT-3, IS29876, IS20697, and IS2787. These lines exhibited higher grain yield even under native N conditions, suggesting their strong capacity for higher N use efficiency. In contrast, low NUE lines were the genotypes whose yield performance was dependent on N availability. Under low N conditions, the least performing lines, considered as N-sensitive lines, included Phule Chitra, SSVMDSORY.5, SSV20064, IS39775, IS4776, DORELKEN, SVD806, GS23, Maldandi, SSM1123, HDW703, IS22325, 97-SB-F5DT-150, GRS1, GS16, SANGATIUI, Macedu, SSM276, SPV2217, and BAHUBANZA3 (Figure 2a).

2.5 | Genome-Wide Association Studies for the Identification of Genes Related to NUE and Associated Traits

In the present study, a total of 1369 MTAs were identified for traits related to NUE and located across the sorghum chromosomes, explaining significant phenotypic variance. Association analysis for DFL, CC, LA, LN, PH, NT, PN, PW, FSY, DSY, GY, TW, and PHI traits under three N conditions identified a significant number of SNPs per trait viz., 31, 30, 29, 32, 32, 204, 61, 147, 28, 109, 184, 182, and 300, respectively (Table S2, Figure 3, Figure S3). Manhattan and Quintile-Quintile (QQ) plots were generated through the SUPER model of GAPIT. For CC, the most significant SNPs were identified on chromosomes 1, 6, 8, and 9 under N0, on chromosomes 2, 3, 4, 6, and 10 under N50, and on chromosomes 1, 2, and 7 under N100. For LA, significant SNPs were identified on intergenic and exonic regions of chromosomes 3, 7, 8, and 10. SNP S10_60562413, an intergenic variant, was observed in both N0 and N100 regimes while significant SNPs for LA were identified on chromosomes 1, 2, 5, 6, 9, and 10 under N50, and on chromosomes 3, 5, 9, and 10 under N100. For LN, most significant SNPs (S1_77012449, S1_72131761, S1_72131726, S1_69406852, S1_69406889, S1_11398982, and S1_11398993) were identified on chromosome 1 under N0 and N50. Other SNPs (S3_14844198, S4_62219103, S9_17559747) were identified on chromosomes 3, 4, and 9 under N0 and N50, respectively. Under N100, SNPs were identified on chromosomes 1, 2, 3, 6, 7, and 10, respectively (Table S2, Figure 3, Figure S3).

For DFL, significant SNPs were identified on chromosomes 1, 2, and 4. SNP S2_61924412 was common to N0 and N100, while SNP S4_15604353 was shared between N0 and N50. Under N50, the most significant SNPs were distributed on chromosomes 1, 4, 7, 8, and 10, whereas under N100, they mapped to chromosomes 2, 3, and 4, respectively. For PH, common SNPs (S3_61949259, S5_46766667, S7_4970164, and S8_39645) were detected under both N0 and N100. SNP S7_64604566 was detected in N0 and N50 regimes, and the intergenic SNP S7_49701640 was found to be consistently detected in all three N regimes. Additionally, SNP S1_66031569 was found to be common under N50 and N100. Across nitrogen dosages, 16 SNPs on chromosome 6 were shared between N0 and N50, 11 SNPs (on chromosomes 1, 3, 4, 5, and 8) were common between N0 and N100, and two loci (S9_50,448,596 and S9_56330993) on chromosome 9 were shared between N50 and N100 (Table S2, Figure 3).

For PN, significant associations were observed under N0 and N50 regimes, where SNPs on chromosome 7 (S7_943417, S7_943455, and S7_946508) and chromosome 3 (S3_67137462) were common. Additional SNPs were identified on chromosomes 1, 3, 6, and 9 under N0, and on chromosomes 1, 2, 3, 4, and 6 under N50. A detailed list of MTAs was enlisted in the Table S2, Figure 3. Significant SNPs for PW were identified across the sorghum chromosomes. Under N0, associations were observed on chromosomes 3, 4, 6, and 10, while N50 and N100 significant SNPs were identified on chromosomes 1, 4, 6, 7, and 8 (Table S2, Figure 3).

For GY, 14 common SNPs were identified under N0 and N50 regimes, primarily located on chromosomes 2 and 3. Between N50 and N100, three SNPs (S7_27327500, S1_68025713 and S7_42117385) were found to be common. For TW trait, four common SNPs (S7_65165549, S7_65165551, S7_65165548 and S7_65165550) were identified under N0 and N50, while N50 and N100 shared associations on chromosomes 1 (S1_79959957, S1_15174725), 5 (S5_5312927), and 10 (S10_54692509). Three SNPs (S6_57648252, S6_57642317, and S9_14969908) were

TABLE 3 | Correlation coefficient analysis of pooled trait data for 186 sorghum accessions evaluated under three N regimes.

Trait	CC	DFL	LA	LN	PHT	NT	PN	PW	GY	FSY	DSY	PHI	HI	TW	GN
(a) N0															
DFL	0.07														
LA	0.08	0.48**													
LN	0.11	0.35**	0.65**												
PHT	−0.01	0.22**	0.12	0.25**											
NT	0.02	−0.10	−0.31**	0.03	0.11										
PN	−0.04	−0.32**	−0.46**	−0.21**	−0.01	0.66**									
PW	−0.10	−0.21**	−0.20**	−0.31**	−0.35**	0.02	0.27**								
GY	−0.09	−0.28**	−0.22**	−0.27**	−0.30**	0.08	0.28**	0.91**							
FSY	−0.04	0.35**	0.31**	0.08	0.27**	−0.08	−0.13	−0.07	−0.10						
DSY	0.06	0.32**	0.38**	0.18*	0.31**	−0.02	−0.09	−0.15*	−0.17*	0.64**					
PHI	0.01	−0.43**	−0.18*	−0.13	−0.10	0.14	0.25**	0.46**	0.69**	−0.09	−0.13				
HI	−0.08	−0.48**	−0.31**	−0.28**	−0.26**	0.08	0.29**	0.60**	0.78**	−0.19**	−0.30**	0.86**			
TW	0.12	−0.24**	0.09	0.05	0.01	−0.18*	−0.15*	0.22**	0.30**	−0.05	0.06	0.49**	0.38		
GN	0.05	−0.05	0.01	0.09	0.13	0.07	−0.01	−0.36**	−0.33**	0.06	0.27**	−0.12	−0.22**	−0.03	
SN	0.07	0.03	0.06	−0.04	−0.39**	0.02	−0.03	0.11	0.09	−0.17*	−0.19**	−0.03	0.02**	−0.06	−0.08
(b) N50															
DFL	0.04														
LA	0.05	0.37**													
LN	0.01	0.28**	0.61**												
PHT	−0.03	0.22**	0.09	0.20**											
NT	−0.06	−0.06	−0.22**	0.20**	0.17*										
PN	−0.13	−0.33**	−0.36**	−0.07	−0.04	0.64**									
PW	−0.14*	−0.25**	−0.02	−0.17*	−0.29**	−0.14	0.09								
GY	−0.14	−0.31**	−0.09	−0.19**	−0.30**	−0.08	0.14	0.93**							
FSY	0.05	0.40**	0.27**	0.25**	0.33**	−0.01	−0.17*	−0.16*	−0.19*						

(Continues)

TABLE 3 | (Continued)

Trait	CC	DFL	LA	LN	PHT	NT	PN	PW	GY	FSY	DSY	PHI	HI	TW	GN
DSY	0.01	0.35**	0.31**	0.20**	0.40**	0.02	−0.12	−0.19**	−0.22**	0.72**					
PHI	−0.13	−0.41**	−0.21**	−0.13	−0.13	0.09	0.23**	0.56**	0.74**	−0.21**	−0.24**				
HI	−0.08	−0.44**	−0.25**	−0.23**	−0.29**	−0.06	0.15*	0.67**	0.81**	−0.37**	−0.42**	0.85**			
TW	−0.01	−0.15*	−0.01	−0.06	−0.04	−0.27**	−0.21**	0.29**	0.34**	0.04	−0.09	0.46**	0.39		
GN	−0.12	−0.04	0.01	0.06	0.11	0.12	0.01	−0.31**	−0.30**	0.09	0.15*	−0.14	−0.22**	0.08	
SN	0.12	0.06	0.16*	−0.03	−0.42**	−0.19**	−0.12	−0.02	−0.06	−0.14	−0.13	−0.20**	−0.10**	−0.10	0.04
(c) N100															
DFL	−0.15*														
LA	−0.16*	0.43**													
LN	−0.11	0.31**	0.56**												
PHT	−0.14	0.19*	0.11	0.20**											
NT	−0.20**	−0.07	−0.27**	0.22**	0.21**										
PN	−0.02	−0.28**	−0.38**	−0.07	0.08	0.63**									
PW	0.02	−0.18*	−0.14	−0.18*	−0.33**	−0.07	0.12								
GY	−0.01	−0.26**	−0.21**	−0.18*	−0.28**	−0.03	0.14*	0.90**							
FSY	−0.04	0.32**	0.29**	0.11	0.35**	−0.03	−0.10	−0.12	−0.12						
DSY	−0.05	0.33**	0.36**	0.09	0.40**	0.01	−0.02	−0.12	−0.14	0.74**					
PHI	−0.06	−0.39**	−0.26**	−0.09	−0.11	0.05	0.16*	0.55**	0.75**	−0.17*	−0.20**				
HI	−0.01	−0.40**	−0.25**	−0.11	−0.25**	−0.04	0.11	0.66**	0.83**	−0.26**	−0.32**	0.85**			
TW	−0.02	−0.04	0.04	−0.01	−0.02	−0.16*	−0.20**	0.33**	0.35**	0.02	0.05	0.41**	0.33		
GN	−0.05	−0.03	0.06	−0.02	0.20**	0.08	0.08	−0.25**	−0.28**	0.08	0.20**	−0.15*	−0.24**	0.11	
SN	0.12	0.02	0.06	−0.03	−0.49**	−0.16*	−0.26**	0.01	−0.09	−0.21**	−0.25**	−0.18*	−0.10**	−0.06	−0.10

Note: Correlation coefficient analysis (a) N0, (b) N50, and (c) N100% of the recommended dose (90 kg/ha).
Abbreviations: CC, SPAD at anthesis stage; DFL, Days to 50% flowering; DSY, dry straw yield (g); FSY, fresh straw yield (g); GN, N content in grain; GY, grain yield (g); HI, harvest index; LA, leaf area; LN, leaf number; NT, number of tillers; PHT, plant height; PN, panicle number; PW, panicle weight (g); SN, N content in straw; TW, test weight (100 seed weight).
*$p = 0.05$.
**$p = 0.001$.

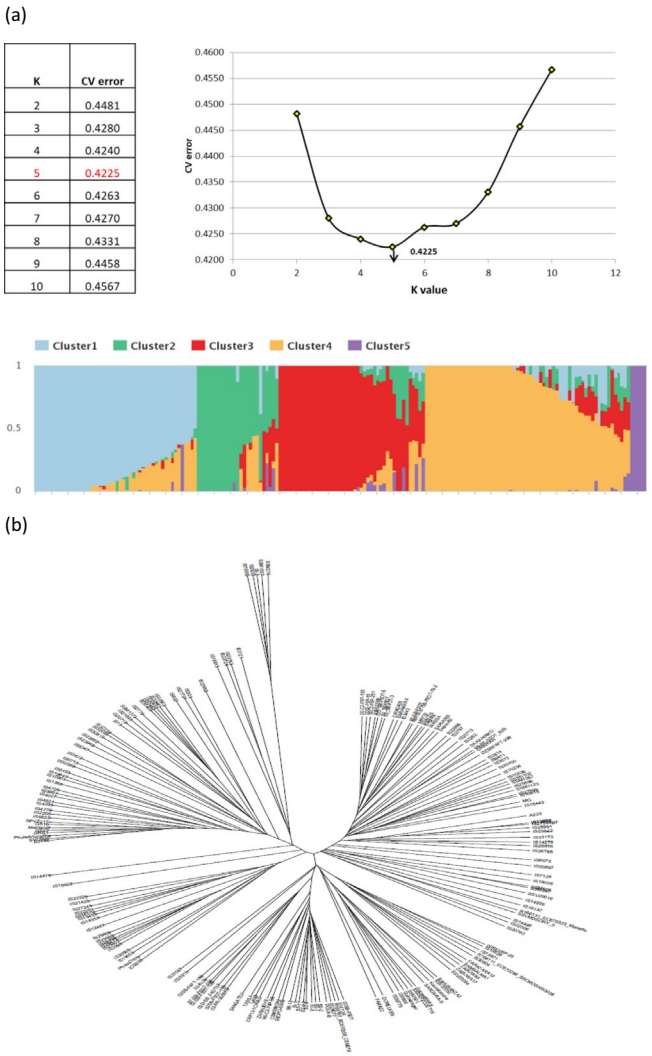

FIGURE 1 | Population structure and phylogenetic analysis (a) Population structure analysis identified five distinct clusters among the sorghum accessions of the study. Here, the *K* value indicates the number of clusters. The optimal K is determined by cross-validation errors (CV errors). (b) Radial phylogenetic tree for analyzing the evolutionary history of the sorghum accessions through an unweighted neighbor-joining method showing five distinct clusters.

common between N0 and N100. Associations for FSY were distributed across all chromosomes, where the SNP S1_57594478 on chromosome 1 was common in N0 and N100 regimes. Common associations for DSY were present on chromosomes 1 and 2 under all nitrogen dosages. Four common SNPs (S1_57683857, S2_12592539, S2_12592561, and S3_61949275) were consistently associated under all three N regimes. Additionally, three SNPs (chromosomes 3 and 10) were common between N0 and N50, while five SNPS (on chromosomes 1, 2, and 5) were found common between N50 and N100. Notably, SNP S7_20117377 was uniquely associated with DSY under N0 and N100 regimes (Table S2, Figure 3).

2.6 | Identification of Putative Candidate Genes

Significant MTAs were aligned using the Sorghum BLAST server, and genes located within 50 kb upstream and downstream window of the MTAs were identified. Genes corresponding to significant SNPs that are in Linkage Disequilibrium (LD) with the specific traits from the sorghum GWAS panel were annotated, and a total of 69 candidate genes associated with N metabolism (uptake, assimilation, and remobilization) were distributed across different chromosomes (Table 4). The majority of the identified genes are known candidate genes of NUE and other abiotic stress-related functional categories, including Nitrate transporter (S1_53455913, S1_53455932), Early nodulin 75-like protein (S7_59397216), Sucrose-phosphatase (S4_48038005), Sucrose-phosphate synthase (S5_12854590), Squamosa promoter-binding-like protein 17 (S2_63584677), WRKY transcription factor 39 (S4_12354578), DNAJ heat shock N-terminal domain-containing protein (S8_60184773, S2_61924412), Aquaporin NIP3-2 (S7_3811837), Putative corA-like Mg^{++} transporter protein (S1_78005543), Potassium channel protein (S9_50448596), Beclin 1 protein (S3_59631616, S3_59627750), Ethylene receptor homologue (S6_3181164), Delayed flowering1 (S2_66204566), Leucine-rich repeat (S2_1024386, S3_62418639), and other transcription factors and stress-responsive candidates such as Dehydrin (PF00257)–(S3_60686805) and NAC-domain containing protein 21/22 (S5_1685470), while few identified genes were of unknown function (Table 4).

2.7 | Transcriptome Analysis of Contrasting Sorghum Genotypes

To identify genotype, N treatment, tissue and time point specific differentially expressed genes, cDNA libraries were prepared from shoot and root samples of high (ICSV745) and low NUE (HDW703) sorghum genotypes collected at two time points (30 min and 6 h) under N0 and N100 regimes. A total of 16 libraries [ICSV745_30m_N0_Shoot,ICSV745_30m_N0_Root,ICSV745_30m_N100_Shoot, ICSV745_30m_N100_Root, ICSV745_6h_N0_Shoot, ICSV745_6h_N0_Root, ICSV745_6h_N100_Shoot, ICSV745_6h_N100_Root,HDW703_30m_N0_Shoot,HDW703_30m_N0_Root,HDW703_30m_N100_Shoot, HDW703_30m_N100_Root, HDW703_6h_N0_Shoot, HDW703_6h_N0_Root, HDW703_6h_N100_Shoot, HDW703_6h_N100_Root] were processed for Illumina RNA sequencing generating 72.1–546.1 million raw reads per library (Table 5). After quality filtering, ~94% of sequences aligned to the sorghum reference genome. Detailed mapping statistics of all libraries are presented in Table 5.

2.7.1 | Differential Transcript Abundance

To capture the expression variation, 24 pairwise comparisons were performed: 8 genotype-specific (high NUE vs. low NUE), 8 treatment-specific (N0 vs. N100), and 8 time point-specific (30 min vs. 6 h) (Table S3a, b, Table 5, Figure 4b–d). Across all comparisons, the number of DEGs ranged from 38 to 3173; the highest number of DEGs (3173) was identified between the root samples collected 30 min after the N100 treatment in ICSV745 and HDW703, followed by 2984 DEGs identified between the root samples collected 30 min after the N0 treatment of ICSV745 and HDW703 (Table S3a, b, Figure S2, Table 5, Figure 4b–d).

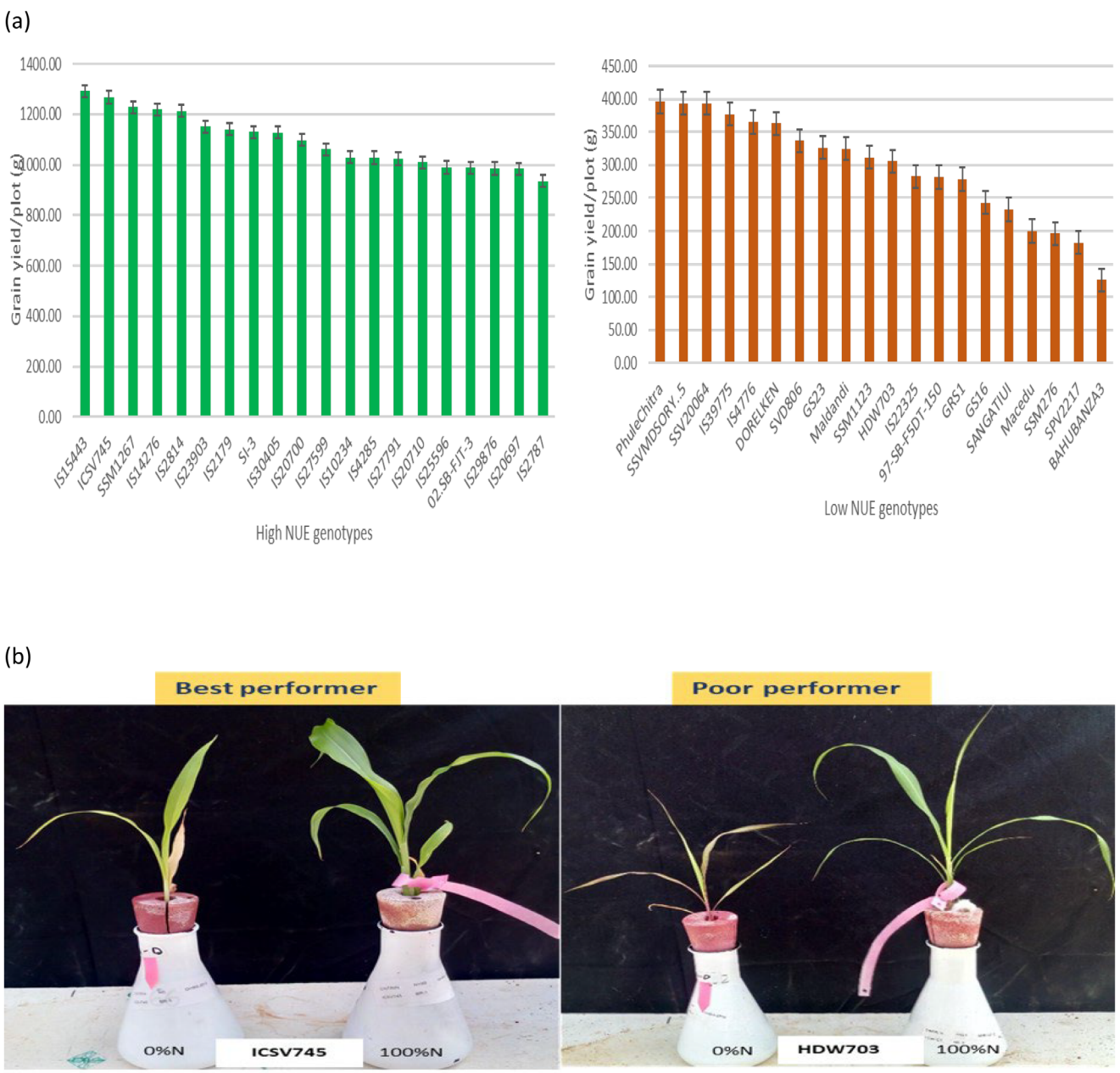

FIGURE 2 | Two-season field evaluation of 186 sorghum accessions for NUE under varying N conditions resulted in the identification of contrasting accessions. (a) Contrasting sorghum accessions for NUE based on grain yield data under N0 conditions. (b) Screening of the selected contrasting sorghum accessions (High NUE: ICSV745 and Low NUE: HDW703) under varied N regimes (0% and 100% of the recommended N) in controlled glass house conditions for RNA sequencing.

2.7.2 | Gene Ontology, Functional Enrichment, and Pathway Analysis

Pair wise comparative analysis of the 24 libraries (Table 3) resulted in the identification of DEGs, which were functionally annotated using Gene Ontology (GO) and enrichment analysis using the R package "topGO" and KOBAS. Among the top 10 biological processes, six GO terms were significantly enriched: organophosphate metabolic process, dephosphorylation, cellular lipid metabolic process, phosphorus metabolic process, phosphate-containing compound metabolic process, and small molecule metabolic process (Table S4a, Figure 4e). For cellular components, the DEGs were highly enriched in cell wall, chloroplast thylakoid, thylakoid, external encapsulating structure, plastid, organelle sub-compartment, extracellular region, chaperonin-containing T-complex, cytoskeleton, and microtubule (Table S4b, Figure 4f). Similarly, the molecular function analysis revealed significant enrichment in carboxypeptidase activity, serine-type carboxypeptidase activity, isomerase activity, serine-type exopeptidase activity, lyase activity, DNA secondary structure binding, minor groove of adenine-thymine-rich DNA binding, monooxygenase activity, and transketolase activity (Table S4c, Figure 4g). The pathway analysis has clustered the enriched GOs into seven major groups, of which the top clusters are biosynthesis of secondary metabolites (enrichment ratio 0.16) and metabolic pathways (enrichment ratio 0.12) (Figure 4h).

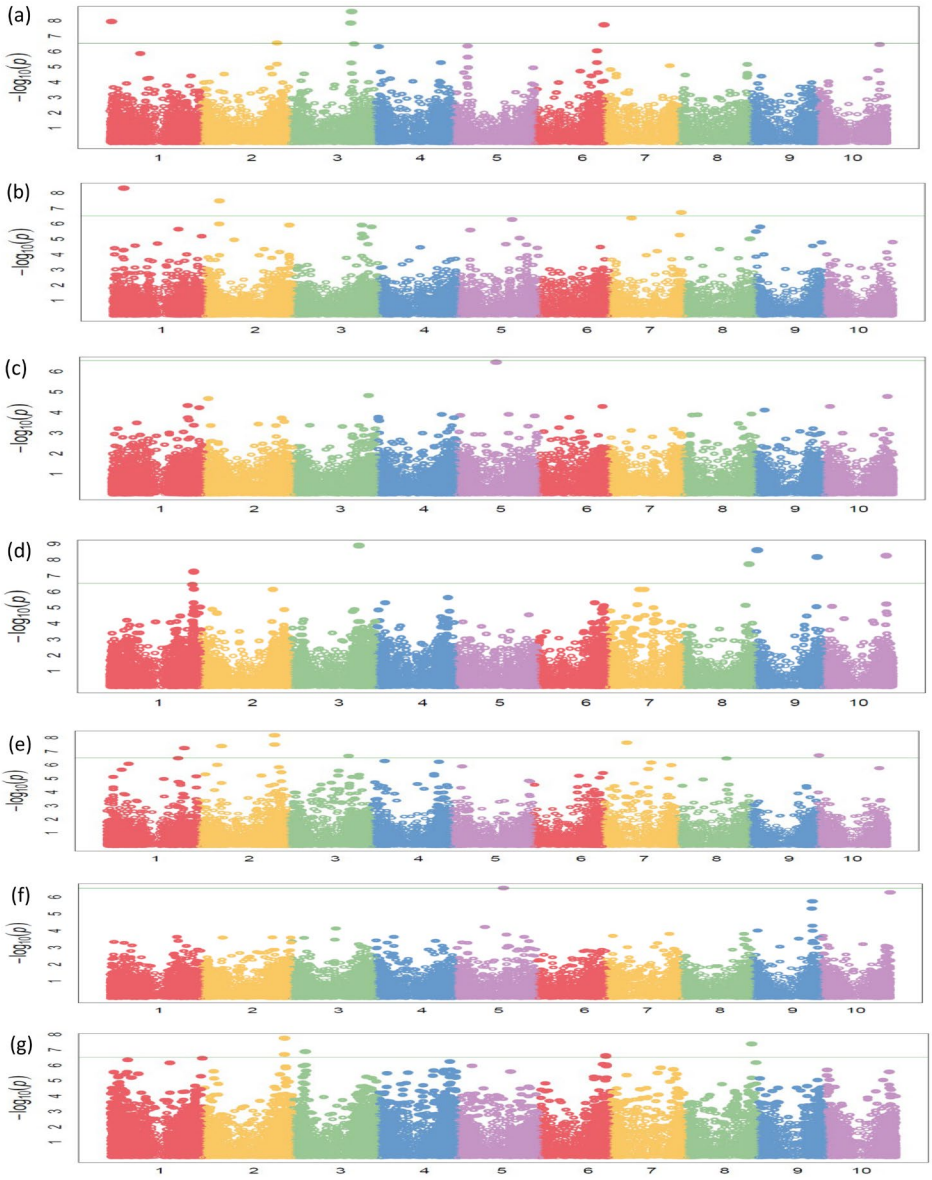

FIGURE 3 | Manhattan plots representing the SNPs in LD with the traits under varying N regimes (N0, N50, and N100% of the recommended dose). Traits include (a) GYLD—Grain Yield (N0), (b) DSYLD—Dry stover yield (N50), (c) LA—Leaf area (N50), (d) PHI—Panicle harvest index (N100), (e) GYLD—Grain Yield (N50), (f) LA—Leaf area (N100), and (g) PHI—Panicle harvest index (N50). In the Manhattan plots, the *x*-axis represents chromosome number, and the coloured dots indicate SNPs specific to each chromosome. The *y*-axis shows the negative logarithm of the association *p*-values, with a horizontal line marking the significance threshold.

2.8 | Identification of Putative Candidate Genes through Integrated GWAS- RNA-Seq Analysis and Comparative Homolog Identification

To corroborate the putative candidate genes identified through GWAS, an integrative analysis was performed by aligning MTAs with DEGs from RNA sequencing. This approach identified 105 genes, distributed across all 10 sorghum chromosomes, that were common to both datasets. The functional annotations of these genes were presented in Table 6, Table S5, and visualized in Figure 5. Additionally, comparative analysis using NCBI TBLASTX further identified putative homologous gene groups across sorghum, rice, wheat, maize, pearl millet, and foxtail millet (Table S5, Figure S1). This analysis revealed 35 reciprocal best-matching gene pairs between sorghum, pearl millet, rice, foxtail millet, wheat, and maize; 38 orthologous gene pairs among sorghum, pearl millet, foxtail millet, wheat, and maize; 2 orthologous gene pairs shared by sorghum, foxtail millet, wheat, and maize; and 1 orthologous gene pair between sorghum, foxtail millet, and pearl millet. Furthermore, 28 unique putative candidate genes were found to be specific to sorghum.

3 | Discussion

Nitrogen Use Efficiency (NUE) in crop plants is a critical determinant of plant growth and yield. Increased application of fertilizer N is not only imposing a financial burden on farmers and governments but also detrimental to soil health and other associated environmental impacts (Galloway et al. 2008). As a complex polygenic trait, improving NUE in staple crops represents a challenging yet remunerative area of research. Understanding

TABLE 4 | Identification of the putative candidate genes associated with NUE and related traits in sorghum through genome-wide association study.

S. No.	SNP	Trait	Treatment	Chromosome	Position	*p* value	Gene	Definition	Pathway
1	S4_62075725	Chlorophyll Content	N100	4	62075725	4.0405E-05	Sobic.004G277800.7	Putative uncharacterized protein	Intracellular protein transport, vesicle-mediated transport
2	S2_61924412	Days to 50% flowering	N0 and N100	2	61924412	8.4766E-05	Sobic.002G227200.4	DNAJ heat shock N-terminal domain-containing protein-like	Peptidyl-diphthamide biosynthetic process from peptidyl-histidine/tRNA wobble uridine modification
3	S10_58288509	Days to 50% flowering	N50	10	58288509	6.1774E-06	Sobic.010G241200.1	Putative uncharacterized protein	Auxin metabolic process/ jasmonic acid metabolic process/regulation of systemic acquired resistance/ response to jasmonic acid
4	S8_61048598	Days to 50% flowering	N50	8	61048598	9.3266E-05	Sobic.008G176300.1	Protein YABBY 6	Transmembrane transport
5	S5_2639021	Days to 50% flowering	N100	5	2639021	3.6758E-05	Sobic.005G029700.1	Ankyrin repeat family protein, putative, expressed	Induced systemic resistance, jasmonic acid mediated signaling pathway
6	S10_55664680	Leaf area	N50	10	55664680	1.6633E-05	Sobic.010G213600.5	Os06g0654300 protein	Cellular response to hydrogen peroxide/cellular response to molecule of bacterial origin/ cellular response to nitric oxide/negative regulation of abscisic acid-activated signaling pathway/negative regulation of ethylene-activated signaling pathway/ protein autophosphorylation/ regulation of stomatal closure/root development

(Continues)

TABLE 4 | (Continued)

S. No.	SNP	Trait	Treatment	Chromosome	Position	*p* value	Gene	Definition	Pathway
7	S9_52022413	Leaf area	N100	9	52022413	4.9919E-05	Sobic.009G163700.1	Os05g0459700 protein	Abscisic acid-activated signaling pathway/mucilage biosynthetic process/ mucilage biosynthetic process involved in seed coat development/ multidimensional cell growth
8	S2_58410744	Leaf area	N100	2	58410744	6.0305E-05	Sobic.002G195700.1	Os09g0400300 protein	Lignin biosynthetic process
9	S6_3181164	Leaf area	N100	6	3181164	6.4181E-05	Sobic.006G018800.1	Ethylene receptor homologue	Regulation of starch metabolic process/ regulation of transcription, DNA-templated
10	S6_3181164	Number of tillers	N0, N50	6	3181164	6.1454E-06	Sobic.006G018800.1	Ethylene receptor homologue	Regulation of starch metabolic process/ regulation of transcription, DNA-templated
11	S3_60581674	Number of tillers	N0	3	60581674	9.4781E-06	Sobic.003G269000.1	Os01g0699600 protein	Activation of protein kinase activity/regulation of mitotic cell cycle/signal transduction by protein phosphorylation/ stress-activated protein kinase signaling cascade
12	S3_60581652	Number of tillers	N0	3	60581652	9.4781E-06	Sobic.003G269000.1	Os01g0699600 protein	Activation of protein kinase activity/regulation of mitotic cell cycle/signal transduction by protein phosphorylation/ stress-activated protein kinase signaling cascade
13	S3_60581681	Number of tillers	N0	3	60581681	9.4781E-06	Sobic.003G269000.1	Os01g0699600 protein	Activation of protein kinase activity/regulation of mitotic cell cycle/signal transduction by protein phosphorylation/ stress-activated protein kinase signaling cascade

(Continues)

TABLE 4 | (Continued)

S. No.	SNP	Trait	Treatment	Chromosome	Position	*p* value	Gene	Definition	Pathway
14	S7_61138589	Number of tillers	N0	7	61138589	3.9628E-05	Sobic.007G178200.1	Putative uncharacterized protein	Endoplasmic reticulum to Golgi vesicle-mediated transport/protein retention in ER lumen
15	S3_65162	Number of tillers	N0	3	65162	7.7454E-05	Sobic.003G000600.2	WRKY transcription factor 1	DNA-binding transcription factor activity/sequence-specific DNA binding
16	S7_5531348	Number of tillers	N50	7	5531348	4.6952E-05	Sobic.007G054500.1	Putative uncharacterized protein	Cotyledon vascular tissue pattern formation/ stem vascular tissue pattern formation/ transmembrane transport
17	S1_7343400	Number of tillers	N50	1	7343400	6.3784E-05	Sobic.001G095500.1	Protein WRKY1	DNA-binding transcription factor activity/sequence-specific DNA binding
18	S9_50448596	Number of tillers	N0, N50 & 100	9	50448596	8.6082E-05	Sobic.009G147500.1	Potassium channel protein ZMK2	Regulation of ion transmembrane transport
19	S4_61818232	Number of tillers	N100	4	61818232	1.7388E-07	Sobic.004G274600.2	MDR-like ABC transporter	Transmembrane transport
20	S7_58295561	Number of tillers	N100	7	58295561	7.9321E-05	Sobic.007G151100.1	12-oxo-phytodienoic acid reductase	Jasmonic acid biosynthetic process/oxylipin biosynthetic process/response to fungus/response to ozone/ stamen development
21	S9_50448596	Panicle number	N0	9	50448596	9.74E-05	Sobic.009G147500.1	Potassium channel protein ZMK2	Regulation of ion transmembrane transport
22	S3_67137462	Panicle number	N0, N50	3	67137462	8.06E-05	Sobic.003G352300.2	Triosephosphate isomerase	Gluconeogenesis/ glyceraldehyde-3-phosphate biosynthetic process/ glycerol catabolic process/ glycolytic process
23	S5_12854590	Panicle weight	N0	5	12854590	3.6726E-05	Sobic.005G089600.1	Sucrose-phosphate synthase	

(Continues)

TABLE 4 | (Continued)

S. No.	SNP	Trait	Treatment	Chromosome	Position	*p* value	Gene	Definition	Pathway
24	S8_60188599	Panicle weight	N0	8	60188599	1.0129E-05	Sobic.008G167800.2	DNAJ heat shock N-terminal domain-containing protein, putative, expressed	
25	S5_1685470	Panicle weight	N50	5	1685470	6.1923E-08	Sobic.005G018700.1	weakly NAC-domain containing protein 21/22, putative, expressed	Regulation of transcription, DNA-templated
26	S2_1024386	Panicle weight	N50	2	1024386	3.9339E-06	Sobic.002G010800.1	NBS-LRR type R protein, Nbs1-Pi2	Defense response
27	S3_5945619	Panicle weight	N50	3	5945619	4.9743E-05	Sobic.003G069700.2	Protein kinase domain (Pkinase)// Leucine Rich Repeat (LRR_1)//Leucine rich repeat N-terminal domain (LRRNT_2)// Leucine rich repeat (LRR_8) (1 of 55)	
28	S2_66204566	Panicle weight	N50	2	66204566	1.572E-06	Sobic.002G280800.1	Delayed flowering1	DNA-binding transcription factor activity
29	S2_54591046	Panicle weight	N100	2	54591046	3.0308E-05	Sobic.002G173000.1	PTHR23155// PTHR23155: SF635—LEUCINE-RICH REPEAT-CONTAINING PROTEIN (1 of 2)	
30	S8_49310934	Fresh stover yield	N0	8	49310934	7.7513E-05	Sobic.008G105100.2	PF04578//PF13968—Protein of unknown function, (DUF594)// Domain of unknown function (DUF4220) (1 of 60)	
31	S4_55647519	Fresh straw yield	N50	4	55647519	3.5521E-05	Sobic.004G205100.1	Glyceraldehyde-3-phosphate dehydrogenase, cytosolic 3	Glucose metabolic process/ glycolytic process

(Continues)

TABLE 4 | (Continued)

S. No.	SNP	Trait	Treatment	Chromosome	Position	*p* value	Gene	Definition	Pathway
32	S7_57320050	Fresh straw yield	N100	7	57320050	1.9246E-05	Sobic.007G143600.1	1.5.1.2—Pyrroline-5-carboxylate reductase/ P5CR (1 of 2)	
33	S3_59631616	Dry straw yield	N50	3	59631616	4.4877E-06	Sobic.003G258300.7	Beclin 1 protein	Autophagosome assembly/ cellular response to nitrogen starvation/late endosome to vacuole transport
34	S3_59,627,750	Dry straw yield	N0	3	59627750	2.6073E-05	Sobic.003G258300.5	Beclin 1 protein	Autophagosome assembly/ cellular response to nitrogen starvation/late endosome to vacuole transport
35	S1_78005543	Dry straw yield	N50	1	78005543	6.348E-06	Sobic.001G512100.1	Putative corA-like Mg++ transporter protein	Magnesium ion transport
36	S3_59627750	Dry straw yield	N0, N50	3	59627750	2.6073E-05	Sobic.003G258300.5	Beclin 1 protein	Autophagosome assembly/ cellular response to nitrogen starvation/late endosome to vacuole transport
37	S2_54591046	Dry straw yield	N0	2	54591046	7.4088E-05	Sobic.002G173000.1	PTHR23155// PTHR23155: SF635—LEUCINE-RICH REPEAT-CONTAINING PROTEIN (1 of 2)	
38	S1_78005543	Dry straw yield	N50	1	78005543	6.348E-06	Sobic.001G512100.1; Sb01g047780	Putative corA-like Mg++ transporter protein	Magnesium ion transport
39	S9_50007571	Dry straw yield	N50	9	50007571	2.8364E-05	Sobic.009G142800.4; Sb09g020790	Putative uncharacterized protein	Amino acid transmembrane transport
40	S1_71702924	Grain Yield	N0	1	71702924	3.9895E-05	Sobic.001G439000.1	AUX1 protein, putative, expressed	Amino acid transmembrane transport
41	S3_53295772	Grain Yield	N0	3	53295772	1.3775E-08	Sobic.003G203200.1	PF06376—Protein of unknown function (DUF1070) (1 of 12)	

(Continues)

TABLE 4 | (Continued)

S. No.	SNP	Trait	Treatment	Chromosome	Position	*p* value	Gene	Definition	Pathway
42	S8_60184773	Grain Yield	N0	8	60184773	2.6876E-05	Sobic.008G167800.1	DNAJ heat shock N-terminal domain-containing protein, putative, expressed	
43	S5_12641179	Grain Yield	N0	5	12641179	4.9479E-05	Sobic.005G088500.1	PF00892—EamA-like transporter family (EamA) (1 of 60)	Transmembrane transporter activity
44	S10_9295410	Grain Yield	N0	10	9295410	9.369E-05	Sobic.010G100800.1	Putative uncharacterized protein	Hyperosmotic salinity response/mannose metabolic process/N-glycan processing/protein deglycosylation/protein N-linked glycosylation
45	S3_62418639	Grain Yield	N50	3	62418639	5.236E-06	Sobic.003G291600.1	PF07714//PF08263//PF13855—Protein tyrosine kinase (Pkinase_Tyr)//Leucine rich repeat N-terminal domain (LRRNT_2)//Leucine rich repeat (LRR_8) (1 of 30)	
46	S2_66204566	Grain Yield	N0 and N50	2	66204566	6.7307E-06	Sobic.002G280800.1	Delayed flowering1	DNA-binding transcription factor activity
47	S3_56243464	Panicle harvest index	N0	3	56243464	5.6702E-07	Sobic.003G225900.1	C2 domain-containing protein-like	Positive regulation of defense response to bacterium, incompatible interaction/positive regulation of response to salt stress/response to salt stress/response to wounding

(Continues)

TABLE 4 | (Continued)

S. No.	SNP	Trait	Treatment	Chromosome	Position	*p* value	Gene	Definition	Pathway
48	S3_68403953	Panicle harvest index	N0	3	68403953	1.519E-06	Sobic.003G368300.1	Leucine zipper protein	Positive regulation of abscisic acid-activated signaling pathway/positive regulation of response to salt stress/positive regulation of response to water deprivation/positive regulation of transcription, DNA-templated
49	S9_42899371	Panicle harvest index	N0	9	42899371	3.0188E-05	Sobic.009G105900.1	Cation chloride cotransporter	Cell volume homeostasis/ chloride ion homeostasis/ chloride transmembrane transport/potassium ion homeostasis/potassium ion import across plasma membrane
50	S3_60686805	Panicle harvest index	N0	3	60686805	2.9163E-06	Sobic.003G270200.1	PF00257—Dehydrin (Dehydrin) (1 of 4)	
51	S4_12354578	Panicle harvest index	N0	4	12354578	4.9654E-06	Sobic.004G117600.1	WRKY transcription factor 39	DNA-binding transcription factor activity/sequence-specific DNA binding/ transcription regulatory region DNA binding
52	S7_59397216	Panicle harvest index	N0	7	59397216	2.7336E-06	Sobic.007G159450.1	Early nodulin 75-like protein	
53	S3_10868383	Panicle harvest index	N50	3	10868383	9.6493E-07	Sobic.003G119800.3	Weakly NAC domain-containing protein 74	Regulation of transcription, DNA-templated
54	S5_12641179	Panicle harvest index	N50	5	12641179	1.0941E-06	Sobic.005G088500.1	PF00892—EamA-like transporter family (EamA) (1 of 60)	Transmembrane transporter activity
55	S4_48038005	Panicle harvest index	N50	4	48038005	2.1815E-06	Sobic.004G151800.1	Sucrose-phosphatase	Sucrose biosynthetic process

(Continues)

TABLE 4 | (Continued)

S. No.	SNP	Trait	Treatment	Chromosome	Position	*p* value	Gene	Definition	Pathway
56	S2_8888563	Panicle harvest index	N50	2	8888563	2.5007E-06	Sobic.002G083100.1	Cation-transporting ATPase	ATPase-coupled cation transmembrane transporter activity/ATP binding/ cadmium ion transmembrane transporter activity/ metal ion binding/zinc ion transmembrane transporter activity
57	S4_57218423	Panicle harvest index	N50	4	57218423	3.2846E-06	Sobic.004G222000.1	Aquaporin PIP2-3	
58	S9_53226072	Panicle harvest index	N100	9	53226072	9.0788E-06	Sobic.009G177400.1	PF07714//PF08263// PF13855—Protein tyrosine kinase (Pkinase_Tyr)//Leucine rich repeat N-terminal domain (LRRNT_2)// Leucine rich repeat (LRR_8) (1 of 30)	
59	S1_53455913	Panicle harvest index	N100	1	53455913	8.5575E-05	Sobic.001G275500.2	Nitrate transporter	Oligopeptide transmembrane transporter activity/ peptide:proton symporter activity/ peptide transmembrane transporter activity
60	S1_53455932	Panicle harvest index	N100	1	53455932	8.5575E-05	Sobic.001G275500.2	Nitrate transporter	Oligopeptide transmembrane transporter activity/ peptide:proton symporter activity/ peptide transmembrane transporter activity
61	S4_2871791	Panicle harvest index	N100	4	2871791	6.7252E-05	Sobic.004G035500.1	Glutamate/malate translocator	Transmembrane transporter activity
62	S3_10868383	Panicle harvest index	N100	3	10868383	5.7137E-05	Sobic.003G119800.3	Weakly NAC domain-containing protein 74	Regulation of transcription, DNA-templated

(Continues)

TABLE 4 | (Continued)

S. No.	SNP	Trait	Treatment	Chromosome	Position	*p* value	Gene	Definition	Pathway
63	S6_56756472	Panicle harvest index	N100	6	56756472	9.8703E-06	Sobic.006G220800.1	Aminomethyltransferase	Glycine decarboxylation via glycine cleavage system
64	S3_66578045	Test weight	N0	3	66578045	2.088E-05	Sobic.003G344400.1	Zinc finger (C3HC4-type RING finger) family protein-like	
65	S7_3811837	Test weight	N0	7	3811837	2.3247E-05	Sobic.007G039500.1	Aquaporin NIP3-2	
66	S2_63584677	Test weight	N50	2	63584677	4.5814E-05	Sobic.002G247800.1	Squamosa promoter-binding-like protein 17	DNA binding, metal ion binding
67	S9_42899371; S9_42899404	Test weight	N100	9	42899371	4.0576E-06	Sobic.009G105900.1	Cation chloride cotransporter	Cell volume homeostasis, chloride ion homeostasis, chloride transmembrane transport, potassium ion homeostasis, potassium ion import across plasma membrane
68	S7_65165550; S7_65165551	Test weight	N0, N50	7	65165550	3.6067E-06	Sobic.007G224100.1	Putative uncharacterized protein	De-etiolation/Protein folding/protein import into chloroplast stroma/response to chlorate/response to heat/response to salt stress/response to water deprivation
69	S10_7869437	Test weight	N0	10	7869437	9.8931E-06	Sobic.010G090500.1	Putative uncharacterized protein	Cortical microtubule organization, gynoecium development, plant-type primary cell wall biogenesis, pollen tube development, pollen wall assembly, protein localization to cortical microtubule cytoskeleton, regulation of microtubule cytoskeleton organization, regulation of root morphogenesis, response to calcium ion, response to water deprivation.

the physiological and molecular basis of NUE under varying N regimes serves as a good starting point for the development of improved crop varieties (Hirel, Chardon, and Durand 2007). Decoding the genetic basis of NUE requires the systematic integration of precise physiological and agronomic data with robust molecular tools and technologies (Srikanth et al. 2016). GWAS is an established approach to dissect the genetic basis of complex and polygenic traits in multiple crops (Wang et al. 2012; Monostori et al. 2017; Rao et al. 2018; Bandyopadhyay et al. 2022; and Zhou et al. 2022). Additionally, transcriptome analysis has proven to be a powerful approach for elucidating plant response to nitrogen status changes at the molecular level; therefore, it is considered a potential tool to mine novel NUE-related loci in crops (Hao et al. 2011; Yang et al. 2015; Quan et al. 2016; Gelli et al. 2017; Bandyopadhyay et al. 2022). These studies have uncovered several novel genomic regions and regulatory pathways that hold potential for improving NUE. This study aimed to understand genotype, N dosage, and season-specific variations related to NUE across a set of 186 diverse sorghum accessions using two seasons of phenotypic data. Furthermore, it seeks to unravel the key genes and regulatory networks related to NUE through integrated GWAS and transcriptome analysis to identify key genes and regulatory networks underlying NUE, ultimately contributing to the development of sorghum varieties with improved nitrogen efficiency.

3.1 | Variability in Physiological, Agronomic, Yield, and N Estimation-Related Traits

Wide variability was observed for the studied traits in 186 diverse sorghum accessions under varied N regimes (0, 50, and 100% of the recommended N) over two seasons, with few exceptions. As nitrogen is a key component of chlorophyll, mean post-flowering chlorophyll content (CC) increased with higher N availability (N50 and N100), consistent with earlier reports in sorghum (Ajeigbe et al. 2018; Bollam et al. 2021). High N availability showed minimal response on days to 50% flowering (DFL) trait in sorghum, aligning with findings in sorghum (Ajeigbe et al. 2018; Bollam et al. 2021), wheat (Guttieri et al. 2017), and mung bean (Achakzai et al. 2012). Sorghum accessions showed N-dependent increases in physiological traits like plant height (PH), leaf area (LA), and leaf number (LN), highlighting the role in facilitating plant growth and development. Yield-related traits, including number of tillers (NT), number of panicles (NP), and panicle weight (PW), also increased with higher N availability. A significant yield penalty in both grain yield (GY) and dry stover yield (DSY) was observed under the N0 compared to the N50 and N100 regimes. However, no significant difference in grain yield was noted between N50 and N100 (Tables 1 and 2). It is well-established that optimal N fertilizer levels stimulate traits such as tiller number, panicle number, and panicle weight, thereby enhancing both grain and stover yield in sorghum (Shamme et al. 2016; Ajeigbe et al. 2018; Gelli et al. 2016; Bollam et al. 2021) and other crops (Laperche et al. 2006; Pan et al. 2016; Srikanth et al. 2016; Yang and Udvardi 2018 and Pujarula et al. 2021) (Tables 1 and 2). Despite the genotypic variability observed, the lack of significant differences in grain yield between the N50 and N100 regimes across seasons may be attributed to the limited ability of some genotypes to utilize excess nitrogen in the soil, suggesting split-dose N application could improve nitrogen recovery and yields.

Higher N availability also enhanced biomass production, with fresh stover yield (FSY) and DSY increasing by ~13% (N50) and ~17% (N100) relative to N0. This enhancement can be attributed to the increased nitrogen availability, which promotes biomass accumulation by strengthening the economic sink capacity of the plants. In contrast, test weight (TW) is not influenced by the N dosage, confirming its varietal dependence (Kanfany et al. 2014). N content in grain and stover (GN and SN) consistently improved with N dosage, reflecting improved remobilization of N into biomass and grain (Tables 1 and 2). These results align with the previous reports, though N content and its relationship to biomass-related traits are highly diverse and vary with genotype, environment, and N application timing (Zhang et al. 2012; Yoshinaga et al. 2013; Shamme et al. 2016; He et al. 2017; Bollam et al. 2021).

3.2 | Correlation Coefficient Analysis

Correlation analysis of traits across seasons and N regimes revealed that grain yield (GY) significantly and positively correlated with panicle traits (PN and PW), HI, and TW, indicating their key role in improving sorghum yield. GY showed a consistent negative correlation with GN under all the treatments and seasons, as previously reported (Sinebo et al. 2004). DSY correlated positively with LA, DFL, LN, PH, and GN under the N0 regime across the seasons, highlighting the importance of morphological traits in stover quality and biomass improvement in sorghum. PHI/HI, a measure of assimilates translocation from source to sink (Li et al. 2012), was positively correlated with GY and PW, and negatively correlated with DSY across the treatments, underscoring its role in yield improvement. Correlation of grain and stover yield and other associated NUE traits was reported to be variable with genotype, N fertilizer dosage, and season-specific variations (Sui et al. 2013; Zhang et al. 2013; Belete et al. 2018). Interestingly, LA and PH significantly correlated with DFL, LN, FSY, and DSY under all the N regimes across the seasons. PN positively correlated with PW, GY, TW, and PHI traits in all regimes and seasons (Table 3). These correlations emphasize the role of morphological and yield traits in nitrogen uptake, assimilation, and remobilization, and provide valuable targets for NUE improvement in sorghum.

3.3 | Population Structure and Diversity Analysis

The 186 sorghum accessions represented wide genetic diversity from Africa and Asia. It is essential to perform structure analysis in natural populations before GWAS to identify and overcome the spurious marker-trait associations (Pritchard et al. 2000; Krill et al. 2010). The hierarchical population structure analysis using 22,439 SNPs grouped accessions into 5 subpopulations ($K = 5$) with some admixture, confirming the genetic diversity (Figure 1a). Phylogenetic analysis using the GBS data also formed five distinct clusters, corroborating the structure analysis (Figure 1b). These findings align with previous reports of strong genetic variability in global sorghum diversity panels (Dossou-Aminon et al. 2015; Satish et al. 2016; Afolayan

et al. 2019; Bollam et al. 2021). The observed genetic diversity of natural populations likely reflects evolutionary patterns, genetic drift, adaptive traits, and environmental heterogeneity (Al Salameen et al. 2020).

3.4 | Contrasting Sorghum Accessions for NUE: Key Resource for NUE Improvement

Based on pooled grain yield data from 186 accessions under low N conditions, contrasting accessions for NUE, viz., high NUE and low NUE lines were identified. Twenty high NUE lines (IS15443, ICSV745, SSM1267, IS14276, IS2814, IS23903, IS2179, SI-3, IS30405, IS20700, IS27599, IS10234, IS4285, IS27791, IS20710, IS25596, 02. SB-FJT-3, IS29876, IS20697, and IS2787) consistently produced higher grain yield under native N conditions, demonstrating their capacity for strong NUE and potential for use in breeding programs. In contrast, low NUE lines require more N fertilizer for their growth and yield performance, with 20 low NUE lines (Phule Chitra, SSVMDSORY.5, SSV20064, IS39775, IS4776, DORELKEN, SVD806, GS23, Maldandi, SSM1123, HDW703, IS22325, 97-SB-F5DT-150, GRS1, GS16, SANGATIUI, Macedu, SSM276, SPV2217, and BAHUBANZA3) under low N conditions (Figure 2a). Among the 20 high NUE genotypes, nine were consistent top-yielders across all three treatments (N0, N50, and N100), confirming their superior performance and plasticity towards N fertilizer dose. Four genotypes (IS15443, IS15526, SSM1267, and IS29876) yielded less under N100 than N50, indicating possible sensitivity to high N levels, while five genotypes (IS14276, IS2814, IS2179, IS10234, and IS27791) displayed consistent yield gains with increasing N. The identification of these contrasting lines provides a valuable resource for dissecting the molecular basis of NUE. Selected high- and low-NUE lines were further used for transcriptome profiling to identify differentially expressed genes and regulatory networks associated with NUE in sorghum.

3.5 | Genome-Wide Association Studies Identified Candidate Genes Associated With N Use Efficiency in Sorghum

GWAS using the SUPER model identified 1369 significant MTAs for physiological, yield, and NUE related traits in sorghum, of which 513, 489, and 367 were detected under N0, N50, and N100 regimes, respectively. These MTAs were spread across all 10 chromosomes (203, 166, 163, 152, 84, 171, 162, 96, 84, and 88 MTAs on Chr 1, 2, 3, 4, 5, 6, 7, 8, 9, and 10, respectively) and explained the phenotypic variance under varying N regimes (Table S2, Table 4, Figure 3). Annotations of trait-linked SNPs revealed candidate genes with functional categories of N uptake, assimilation, remobilization, and stress tolerance. Notable examples include nitrate transporters (SNPs, S1_53455913 and S1_53455932), a known candidate for nitrate absorption from the soil and its translocation to different plant parts; additionally, it is also involved in nitrate assimilation by integrating with carbon skeletons for amino acid synthesis (Feng et al. 2011; Xu et al. 2012). Cor A Mg^{2+} transporters (S1_78005543) associated with Mg ion transport across the cell membranes (Guskov et al. 2012), and potassium channel proteins encoded by SNP S9_50448596, play an important role in the maintenance of ion homeostasis and stress tolerance (Kumar et al. 2022). Other important candidates were DNAJ heat shock proteins (S2_61924412, S8_60184773) known for the maintenance of cellular homeostasis and stress tolerance (Mulaudzi-Masuku et al. 2015). Early nodulin 75-like proteins encoded by SNP S7_59397216 are transmembrane proteins with transporter activity (Denancé et al. 2014). SNP S6_3181164 encodes for ethylene receptor homologue (Sobic.006G018800.1) associated with the regulation of starch metabolic process (Yang et al. 2015). DSY trait-linked SNPs (S3_59631616, S3_59627750) encoding Beclin 1 protein of Arabidopsis are known for their role in the cellular response to nitrogen starvation and inducing male sterility in plants (Singh et al. 2010).

Genes affecting yield and carbon partitioning were also identified, panicle weight-linked SNP S4_48038005 encoding Sucrose-phosphatase and S5_12854590 encoding Sucrose-phosphate synthase (SPS), two key enzymes involved in the catalysis of the final step of the sucrose biosynthesis pathway, which regulates sucrose content in plants (Anur et al. 2020). Squamosa promoter-binding-like protein 17 (S2_63584677) is a known candidate gene regulating the ideal plant architecture, panicle branching, higher grain productivity, and reduction in tiller number in rice (Jiao et al. 2010; Luo et al. 2012; Srikanth et al. 2016). Stress-responsive transcription factors such as WRKY (S1_7343400, S3_65162, S4_12354578), NAC-domain proteins (S3_10868383, S5_1685470), a key candidate for regulating plant stress response-related transcriptional reprogramming, are strongly linked to biomass and yield potential in sorghum (Xia et al. 2018; Zhao et al. 2007), xylem development in Arabidopsis (Zhao et al. 2007), and YABBY6 (S8_61048598), which is involved in growth and transmembrane transport of molecules (Jie et al. 2022) were enriched. Aquaporin PIP2-3 (S4_57218423) and Aquaporin NIP3-2 (S7_3811837 SNPs) regulate the cellular localizations and selective transport of water and other molecules across plant parts (Maurel et al. 2015), while dehydrin (S3_60686805) plays an important role in establishing protective responses to dehydration and maintains plant abiotic stress tolerance (Liu et al. 2017). Additional candidates included DSY-linked SNP S1_71702924, encoding Sobic.001G439000.1 gene (AUX1 protein), and GY-linked SNP S9_50007571 encoding Sobic.009G142800.4; Sb09g020790 genes associated with amino acid transmembrane transport (Swarup and Bhosale 2019). Glutamate/malate translocator (S4_2871791) is associated with transmembrane transporter activity. GY, PW, PHI traits linked SNPs encoding for Leucine-rich repeats (LRR) motif proteins (S2_1024386, S2_54591046, S3_62418639, S3_5945619, S9_53226072), confer resistance towards biotic stresses in plants (Ng and Xavier 2011). Sobic.007G224100.1 (SNPs S7_65165550; S7_65165551) gene is involved in response mechanisms to chlorate, heat, salt stress, and water deprivation. Delayed flowering1 (S2_66204566) gene associated with leucine zipper protein mediates floral induction on the shoot apex and delays flowering in plants (Muszynski et al. 2006). Zinc finger (C3HC4-type RING finger) family (S3_66578045) is involved in drought stress resistance in plants (Han et al. 2020). All these results clearly indicate that NUE is a complex, polygenic trait regulated by multiple QTLs and gene families integrating N metabolism, stress adaptation, plant development, and yield improvement. The identified candidate genes provide valuable targets for improving NUE and stress resilience in sorghum, particularly under low-nitrogen conditions (Table S2, Table 4, Figure 3).

3.6 | Transcriptome Analysis of Contrasting Sorghum Accessions Identified Differentially Expressed Genes

Transcriptome analysis of shoot and root samples from contrasting sorghum (high [ICSV745] and low NUE [HDW703]) accessions grown under N0 and N100 conditions identified about 10,800 differentially expressed genes, of which 8661 gene transcripts were identified in root samples (16 combinations), whereas 2229 gene transcripts were identified in shoot samples (16 combinations). The higher number of DEGs is expected as the analysis is based on 24 pairwise comparisons (Table S3a, b, Table 5, Figure 4a) in three broad categories: (i) genotype-specific (High NUE vs. Low NUE), (ii) treatment specific (N0 vs. N100), and (iii) time point specific (30 min vs. 6 h). The higher proportion of root-specific DEGs is indicative of tissue-specific functional specialization, consistent with similar observations in maize, where roots (primary, seminal, and crown roots) show higher DEG counts than aerial tissues (Tai et al. 2016). Most DEGs were annotated as putative uncharacterized proteins or genes related to housekeeping functions and secondary metabolite synthesis. However, a substantial number were associated with NUE-related traits, abiotic/biotic stress responses, and gene regulation pathways known to influence the expression of a large number of downstream genes (84; 85; 86; 87; 88) (Cohen et al. 2010; Kakumanu et al. 2012; Johnson et al. 2014; Gelli et al. 2016; Drobnitch et al. 2021).

Several candidate genes were differentially expressed between high and low NUE genotypes (Genotype-specific DEGs) (Table 5, Figure 4b, Table S3a, b). Notable genes include Sobic.006G230800, encoding N-MYC DOWNREGULATED-LIKE1 (NDL1) protein homolog, which modulates root auxin transport and may contribute to differences in root biomass under varied N regimes (Mudgil et al. 2009), Another important candidate gene, Sobic.003G360600, encoding cytochrome P450 (CYP) enzymes, also showed genotype-specific expression. Cytochrome P450s are central to oxidation–reduction reactions by stimulating dioxygen (Isin and Guengerich 2007), stress-induced anthocyanin biosynthesis (Morant et al. 2003), and plant metabolic diversification (Hansen et al. 2021). Four CYPs were reported to be upregulated under N stress in rice (Cai et al. 2012). Other DEGs include Sobic.007G080780 encoding receptor-like protein EIX2 (Drobnitch et al. 2021), Sobic.004G164200 encoding Copper transport protein (Ali 2019), Sobic.005G209200 coding for transcription factor, a GRAS family proteins/scarecrow-like protein 9 (http://planttfdb.gao-lab.org/tf.php?sp=Sbi&did=Sobic.005G209200.1.p), Sobic.001G177000 encoding Chlorophyll a-b binding protein 151 homolog (Sbi-MIR2610b), and Sobic.005G043800, a Major Facilitator Superfamily protein involved in solute transport and pathogen resistance (Diao et al. 2021). Sobic.008G142400 encodes triterpenoid synthase gene involved in sterol biosynthesis (Busta et al. 2021).

Treatment-specific (N0 vs. N100 treatments) DEGs (Table 5, Figure 4c, Table S3a, b) include high-affinity nitrate transporter (NRT) genes (Sobic.004G009500) involved in nitrate uptake and its translocation between different parts of the plant (Boatwright et al. 2022). As expected, these genes were more highly expressed in the roots of the high NUE genotype (ICSV 745) under N-limited conditions, consistent with previous findings in Arabidopsis and sorghum (Gelli et al. 2014). Another important gene was Sobic.004G180000, encoding a Squamosa promoter-binding protein-like (SBP domain) transcription factor, involved in starch metabolism and panicle branching in cereal crops, and is known to be a major candidate gene associated with NUE and grain filling (Jiao et al. 2010; Luo et al. 2012; Srikanth et al. 2016). Interestingly, the SPB domain was differentially expressed in the root samples of the low NUE genotype (HDW 703). Other differentially expressed genes include Sobic.002G050300 coding for lipid-transfer protein/seed storage 2S albumin superfamily protein (Calabrese 2016), Sobic.002G421300 encoding hydroxyproline-rich glycoprotein family protein (Willig 2021), and Sobic.001G212000 encoding ABA-responsive protein homolog involved in drought stress-responsive mechanisms (Singh and Laxmi 2015). Another important gene, Sobic.002G261500 encoding for auxin-induced in the root (*AIR12*) protein, is differentially expressed in root samples of the low NUE (HDW 703) genotype. AIR 12 proteins are known to be involved in the adaptation to N-limited conditions (Krapp et al. 2011; Geldner et al. 2001; Gelli et al. 2014), and the differential expression of these genes in the low NUE genotype possibly reflects variations in root mass development under limited N conditions.

Time point specific (30 min vs. 6 h) DEGs (Table 5, Figure 4d, Table S3a, b) revealed several candidate genes, including thiamine thiazole synthase encoded by Sobic.002G384400 (Ali 2019), Sobic.001G395900 gene coding nicotianamine synthase (ZmNAS2) protein homolog involved in the production of nicotianamine (Mizuno et al. 2003). *Sobic.004G340200 encoding Cinnamoyl-CoA reductase*, an important enzyme in the lignin biosynthesis pathway, is also an effector of small GTPase Rac in defense signalling in rice and other crops (Kawasaki et al. 2006). Other DEGs include Sobic.002G384400 encoding metabolic process and oxidation–reduction GO categories (Kianifariz 2017), Sobic.006G074200 gene encoding lipid metabolism and transfer. Sobic.009G154700 encoding Ferredoxin-6, chloroplast precursor homolog. Sobic.005G110508 encoding NB-ARC domain-containing disease resistance protein. These genes are largely involved in metabolic processes, redox homeostasis, defense responses, and nutrient stress adaptation, highlighting the dynamic transcriptional reprogramming that occurs at different time points under contrasting N conditions.

3.7 | Gene Ontology Enrichment and Pathway Analysis

Differentially expressed transcripts in high (ICSV745) and low (HDW703) NUE genotypes were processed for the gene ontology enrichment analysis. Six GO terms were significantly enriched, which include organophosphate metabolic process, dephosphorylation, cellular lipid metabolic process, phosphorus metabolic process, phosphate-containing compound metabolic process, and small molecule metabolic process (Table S4, Figure 4e). In terms of cellular components, DEGs were highly enriched in the top 10 significant GO terms: cell wall, chloroplast thylakoid, thylakoid, external encapsulating structure, plastid, organelle sub-compartment, extracellular region, chaperonin-containing T-complex, cytoskeleton, and microtubule (Table S4, Figure 4f). Similarly, molecular function also shows significant enrichment in the top 10 GO

TABLE 5 | RNA sequencing of contrasting sorghum accessions: Details of comparative analysis along with differentially expressed gene (DEG) statistics.

Category	Sample	UP regulated genes	Down regulated genes	Total DEGs
Analysis 1- High NUE vs. Low NUE (genotype)	ICSV745_30m_N0_Shoot (1) vs. HDW703_30m_N0_Shoot (9)	75	172	247
	ICSV745_30m_N0_Root (2) vs. HDW703_30m_N0_Root (10)	2301	683	2984
	ICSV745_30m_N100_Shoot (3) vs. HDW703_30m_N100_Shoot (11)	74	179	253
	ICSV745_30m_N100_Root (4) vs. HDW703_30m_N100_Root (12)	2284	889	3173
	ICSV745_6h_N0_Shoot (5) vs. HDW703_6h_N0_Shoot (13)	61	224	285
	ICSV745_6h_N0_Root (6) vs. HDW703_6h_N0_Root (14)	69	145	214
	ICSV745_6h_N100_Shoot (7) vs. HDW703_6h_N100_Shoot (15)	71	194	265
	ICSV745_6h_N100_Root (8) vs. HDW703_6h_N100_Root (16)	90	107	197
Analysis 2- N0 vs. N100 (treatment)	ICSV745_30m_N0_Shoot (1) vs. ICSV745_30m_N100_Shoot (3)	3	51	55
	ICSV745_30m_N0_Root (2) vs. ICSV745_30m_N100_Root (4)	54	8	62
	ICSV745_6h_N0_Shoot (5) vs. ICSV745_6h_N100_Shoot (7)	65	2	67
	ICSV745_6h_N0_Root (6) vs. ICSV745_6h_N100_Root (8)	23	15	38
	HDW703_30m_N0_Shoot (9) vs. HDW703_30m_N100_Shoot (11)	57	138	196
	HDW703_30m_N0_Root (10) vs. HDW703_30m_N100_Root (12)	456	59	515
	HDW703_6h_N0_Shoot (13) vs. HDW703_6h_N100_Shoot (15)	83	47	130
	HDW703_6h_N0_Root (14) vs. HDW703_6h_N100_Root (16)	124	134	258
Analysis 3–30 min vs. 6 h (time point)	ICSV745_30m_N0_Shoot (1) vs. ICSV745_6h_N0_Shoot (5)	52	93	145
	ICSV745_30m_N0_Root (2) vs. ICSV745_6h_N0_Root (6)	88	50	138
	ICSV745_30m_N100_Shoot (3) vs. ICSV745_6h_N100_Shoot (7)	99	7	106
	ICSV745_30m_N100_Root (4) vs. ICSV745_6h_N100_Root (8)	48	203	251
	HDW703_30m_N0_Shoot (9) vs. HDW703_6h_N0_Shoot (13)	72	237	309
	HDW703_30m_N0_Root (10) vs. HDW703_6h_N0_Root (14)	81	99	180
	HDW703_30m_N100_Shoot (11) vs. HDW703_6h_N100_Shoot (15)	127	44	171
	HDW703_30m_N100_Root (12) vs. HDW703_6h_N100_Root (16)	177	474	651

categories, such as carboxypeptidase activity, serine-type carboxypeptidase activity, isomerase activity, serine-type exopeptidase activity, lyase activity, DNA secondary structure binding, minor groove of adenine-thymine-rich DNA binding, monooxygenase activity, and transketolase activity (Table S4, Figure 4g). The pathway analysis has clustered the enriched GOs into seven groups, of which the top cluster has biosynthesis of secondary metabolites (enrich ratio 0.16) and metabolic pathways (enrich ratio 0.12) (Figure 4h).

3.8 | Identification of Key Candidate Genes for NUE, N Stress Tolerance, and Biotic Stress Through an Integrated GWAS and RNA Seq Data

To ascertain commonalities, we cross-referenced GWAS-derived MTAs and RNA-Seq DEGs and identified 105 candidate genes distributed across all 10 sorghum chromosomes. The functional annotation highlighted genes linked to NUE, grain filling, and stress resistance. F-box genes (Sobic.002G106200; Sobic.005G077900) on Chr 2 and 5 encode F-box proteins (FBPs), which play a crucial role in nitrogen metabolism, influencing N uptake, transport, assimilation, and signaling plant growth, development, and stress resilience (Zhang et al. 2021). FBPs are key components of the SCF (SKP1–Cullin–F-box) E3 ubiquitin ligase complex; these proteins play a critical role in N metabolism by mediating targeted degradation of Nitrate Transporters (NRTs) and Ammonium Transporters (AMTs) to fine-tune nitrogen uptake through the ubiquitin-proteasome system (Meijón et al. 2014). F-box proteins also modulate Nitrate Reductase (NR) and Glutamine Synthetase (GS) activity, ensuring efficient nitrogen assimilation (Zhao et al. 2024).

Protein kinases (Sobic.002G172100, Sobic.002G172200) are major candidates in signal transduction pathways,

regulating stress responses (Zhu 2016; Chen et al. 2021). While Sobic.002G343600 encodes Leucine-rich repeats (LRR) motif proteins, connected with pathogen response, and confers resistance towards biotic stresses (Ng and Xavier 2011). ATP-binding Cassette (ABC) transporters (Sobic.003G216300; Sobic.007G095100) on Chr 3 and 7 were identified. These transporters are major protein families (> 100 ABC transporters) present in the plant genome. ABC transporters are membrane-intrinsic primary active pumps, driven by ATP hydrolysis, that facilitate the movement of nitrate (NO_3^-), ammonium (NH_4^+), amino acids, and peptides across cell membranes. These transporters are essential for N uptake, assimilation, translocation, and stress adaptation and also contribute to both biotic and abiotic stress tolerance (Tegeder and Hammes 2018; Do et al. 2021). On Chr 4, the Sobic.004G127200 gene encoding xyloglucan endotransglucosylase/hydrolase (XTH) was identified, and it is widely present in plant cells and is involved in cell wall reconstruction and stress resistance in plants (Cheng et al. 2021). The Sobic.004G133500 gene encoding bi-directional sugar transporter (SWEET) facilitates the movement of sugars across cell membranes according to the concentration gradient. While their primary function is sugar transport, they also play a significant role in N metabolism by regulating the balance between carbon and nitrogen. Additionally, they also contribute to abiotic stress tolerance (Kryukov et al. 2021).

Sobic.004G269900, encoding WRC domain proteins (NIN-like proteins, NLPs), are the plant-specific growth-regulating factors (GRFs) critical for regulating NUE and N stress tolerance. These proteins entail a nuclear localization signal and DNA-binding zinc finger motif and are an integral part of N signalling pathways, playing a major role in both uptake and assimilation of N, thereby influencing plant growth, yield, and stress resilience (Huang et al. 2021). The rice ortholog *OsNLP4* is reported to orchestrate the expression of major nitrogen uptake, assimilation, and signalling genes by binding to nitrate-responsive cis-elements in their promoters (Wu et al. 2021). On Chr 5 and 6, Sobic.005G052500 and Sobic.006G045400 encode amino acid trans domain containing protein and amino acid selective channel proteins, which are amino acid transporters, key mediators of N distribution in plants. These transporters are critical for root N uptake, xylem-phloem translocation, intracellular movement, phloem, flower, and seed development (Yao et al. 2020). On Chr 7, Sobic.007G101500, encoding glucose-1-phosphate adenylyl transferase (AGPase), is a key enzyme in starch and sucrose metabolism. It catalyzes ADP-glucose synthesis, the first step in the starch biosynthesis pathway, providing the substrate for starch synthase to elongate the glucan chain (Preiss 2009). AGPase plays a key regulatory role in controlling carbon flux toward starch accumulation, thereby influencing both yield and biomass production (Geigenberger 2011). Additionally, its role in stress adaptation has been established, as it enhances carbon allocation efficiency under changing environmental conditions (Tetlow and Emes 2017). The geneSobic.007G101800, encoding phosphofructokinase (PFK) domain-containing protein, is an important regulatory enzyme in glycolysis. It catalyzes the phosphorylation of fructose-6-phosphate to fructose-1,6-bisphosphate, a critical step in sugar metabolism (Fernie et al. 2020). PFK's function is tightly linked to nitrogen metabolism, as carbon availability directly affects nitrogen assimilation and use efficiency (NUE); additionally, it contributes to abiotic stress tolerance, including resistance to hypoxia, cold, and drought (Wang et al. 2021).

On Chr 8, Sobic.008G100300 gene encodes a PUM-HD domain-containing protein involved in plant development and stress response by regulating stress-responsive gene networks and hormone signaling pathways through post-transcriptional gene expression (Huh 2021). Additionally, these genes play a major role in maintaining cellular homeostasis under adverse conditions.

Sobic.008G135800 gene encoding Lipase GDSL domain-containing protein, a diverse group of esterases/lipases involved in lipid metabolism, plant development, and stress response mechanisms (Xu et al. 2022). On Chr 9, Sobic.009G111200 gene encoding APETALA2/ethylene response factor (AP2/ERF), part of a major transcription factor (TF) family involved in nitrogen metabolism. It regulates NRTs and AMTs gene expression, influencing nutrient uptake and regulating the expression of nitrate reductase (NR) and glutamine synthetase (GS), which are critical for N assimilation (Cao et al. 2020). Additionally, these TFs also modulate root architecture and nitrate-responsive pathways, contributing to improved nitrogen use efficiency (NUE) and stress adaptation (Meng et al. 2021). Hydroxysteroid dehydrogenase (HSD) gene (Sobic.009G243400) is associated with enhanced biomass and grain yield, together with higher tolerance to salt and AB-mediated seed dormancy in transgenic plants (Li et al. 2007). On Chr 10, *Sobic.010G274400* gene encoding *FAD-binding PCMH-type domain-containing protein and is associated with* P accumulation in wheat (Alomari et al. 2021). Though many known candidate genes and protein candidates identified in this study are known to play a role in N uptake, assimilation, and remobilization and stress resilience, still there is a need for more discussion about the molecular mechanisms underlying N use efficiency across crop species. Notably, transporter genes such as Sobic.003G216300, Sobic.007G095100 (ATP-binding Cassette (ABC) transporters), Sobic.004G133500 (bi-directional sugar transporter-SWEET), Sobic.005G052500, Sobic.006G045400 (Amino acid selective channel proteins; Amino acid transporters), starch and sucrose metabolism genes Sobic.007G101500 (Glucose-1-phosphate adenylyl transferase), Sobic.008G135800 (Lipase GDSL domain-lipid transport) play an essential role in C/N partitioning. Furthermore, genes such as Sobic.009G243400 (hydroxysteroid dehydrogenase (HSD)), Sobic.008G100300 (plant PUM-HD), Sobic.007G101800 (phosphofructokinase (PFK) domain), Sobic.004G269900 (WRC domain), Sobic.002G106200, Sobic.005G077900 (F-box genes), and transcription factors Sobic.009G111200 (APETALA2/ethylene response factor (AP2/ERF)) respectively have been implicated in N sensing, N/C partitioning and transport, starch and glucose metabolism, grain filling, and other abiotic stress resistance factors, all of which ultimately influence yield outcomes (Table 6, Table S5).

Therefore, several candidate genes identified in this study have direct roles in nitrogen uptake, transport, or signalling, underscoring their practical relevance for sorghum improvement. For example, loci encoding high-affinity nitrate transporters (NRT2 family) and ammonium transporters (AMT1 family) are central to root nitrogen acquisition under low-N conditions (Xu

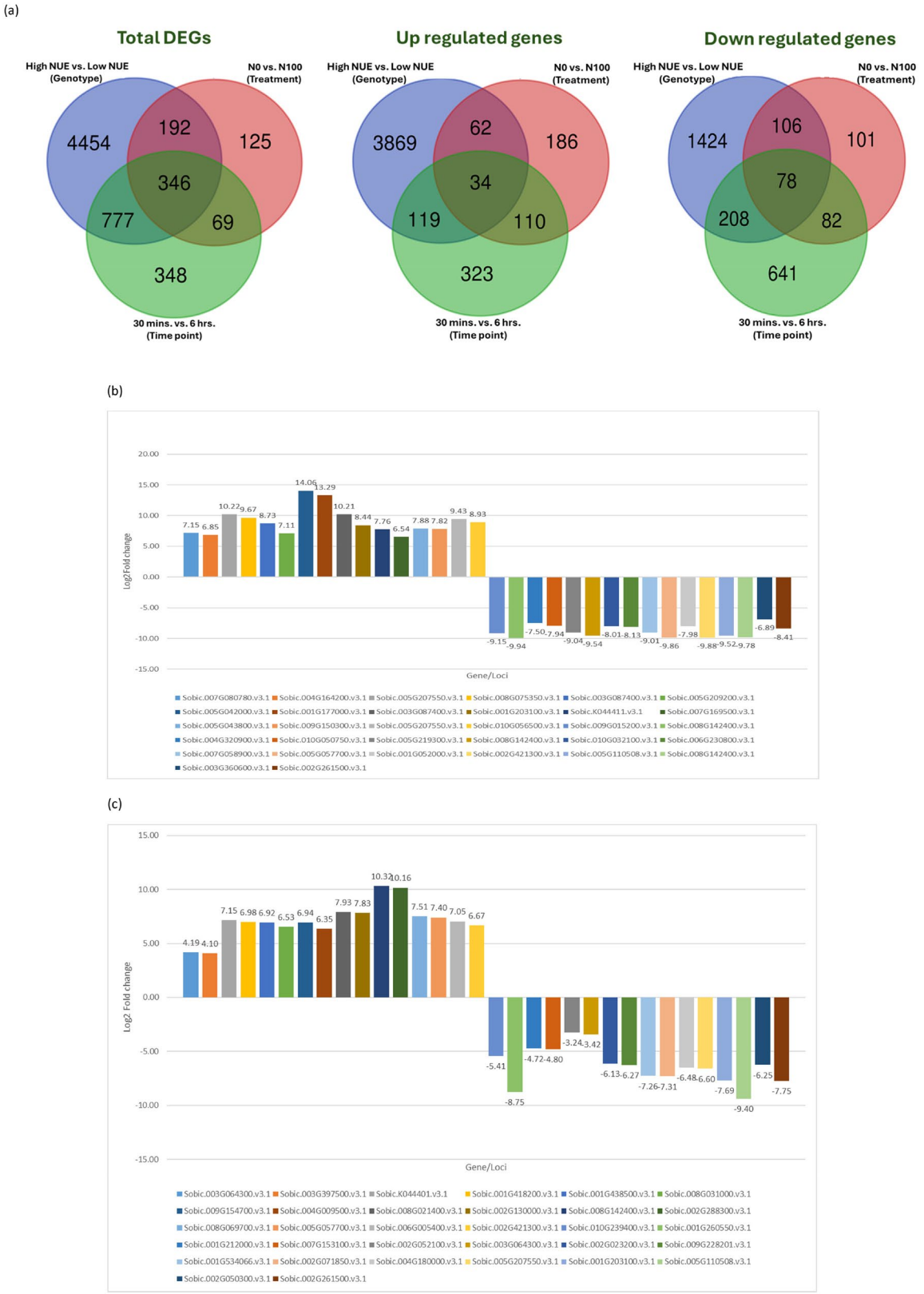

FIGURE 4 | RNA sequencing of contrasting sorghum accessions (High NUE: ICSV745 and Low NUE: HDW703) under varied N regimes (0% and 100% of the recommended N [90 kg/ha]) and time points (Tissue collection @30 min and 6 h after N induction) exhibited interesting findings; these are presented in the figures. (a) Statistics on total DEGs, up-regulated genes, and down-regulated genes. Top up and down regulated genes (DEGs) in each analysis category along with fold change details (b) High NUE versus Low NUE (Genotype), (c) N0 vs. N100 (Treatment), (d) 30 min versus 6 h (time point). In this *x*-axis represents gene ID and the *y*-axis represents fold change. Highly enriched genes for different (e) cellular processes, (f) biological processes and (g) molecular processes. (h) Gene enrichment analysis bar plot showing highly enriched gene functions (*y*-axis), each row represents an enriched function, and the length of the bar represents the enrich ratio (*x*-axis), which is calculated as "input gene number" "background gene number."

(d)

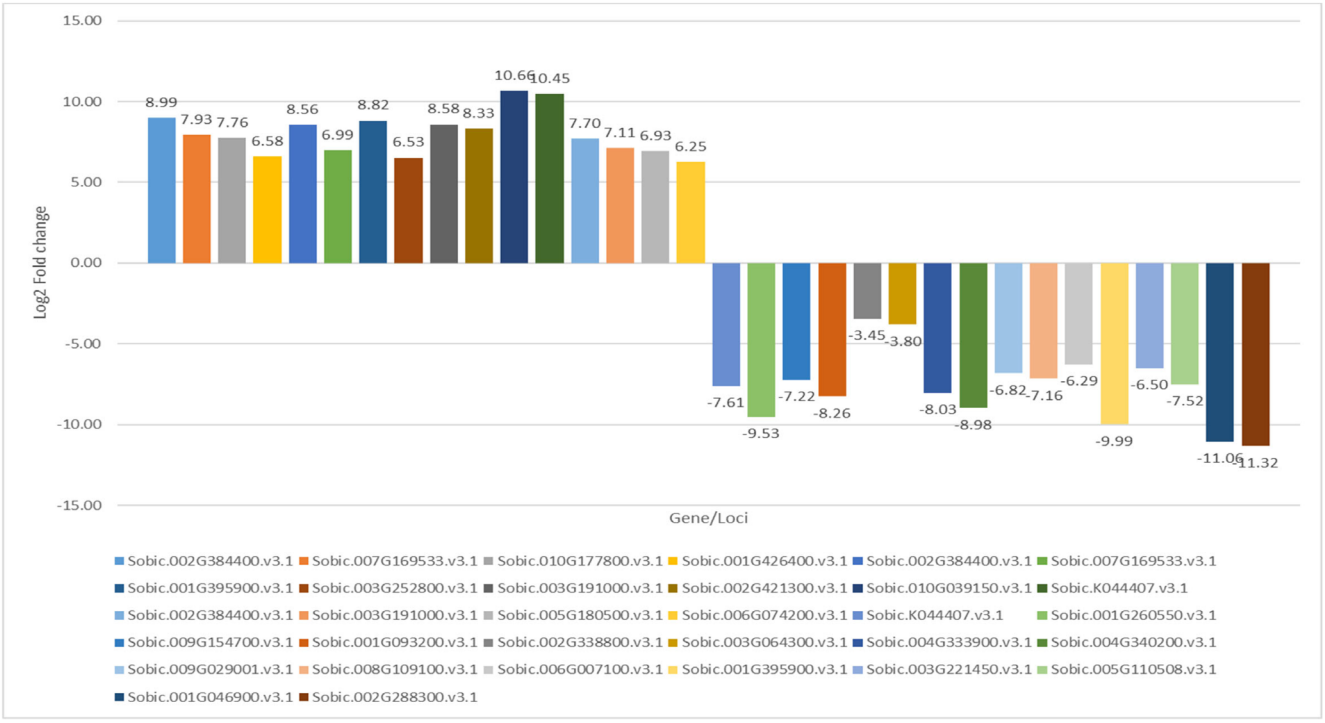

(e)

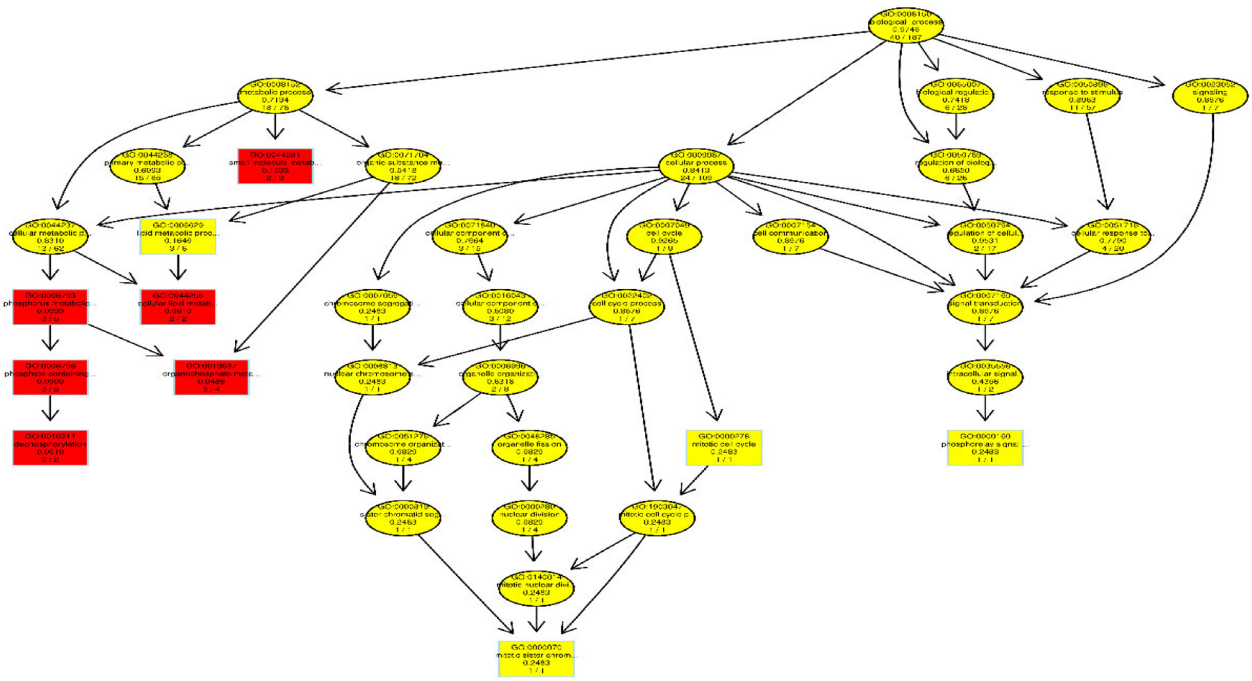

FIGURE 4 | (Continued)

et al. 2012; Garnett et al. 2015). Genes involved in nitrate assimilation, such as nitrate reductase (NR) and glutamine synthetase (GS), facilitate the incorporation of inorganic nitrogen into amino acids, a key step in nitrogen metabolism (Hirel, Chardon, and Durand 2007). We also detected candidate genes encoding protein kinases and transcription factors (e.g., NLP, MYB) that are known to modulate nitrogen-responsive gene networks and signalling cascades (Konishi and Yanagisawa 2013; Alvarez et al. 2014). The functional annotation of these genes highlights their potential as breeding targets for developing nitrogen-efficient sorghum varieties capable of maintaining yield with reduced fertilizer inputs.

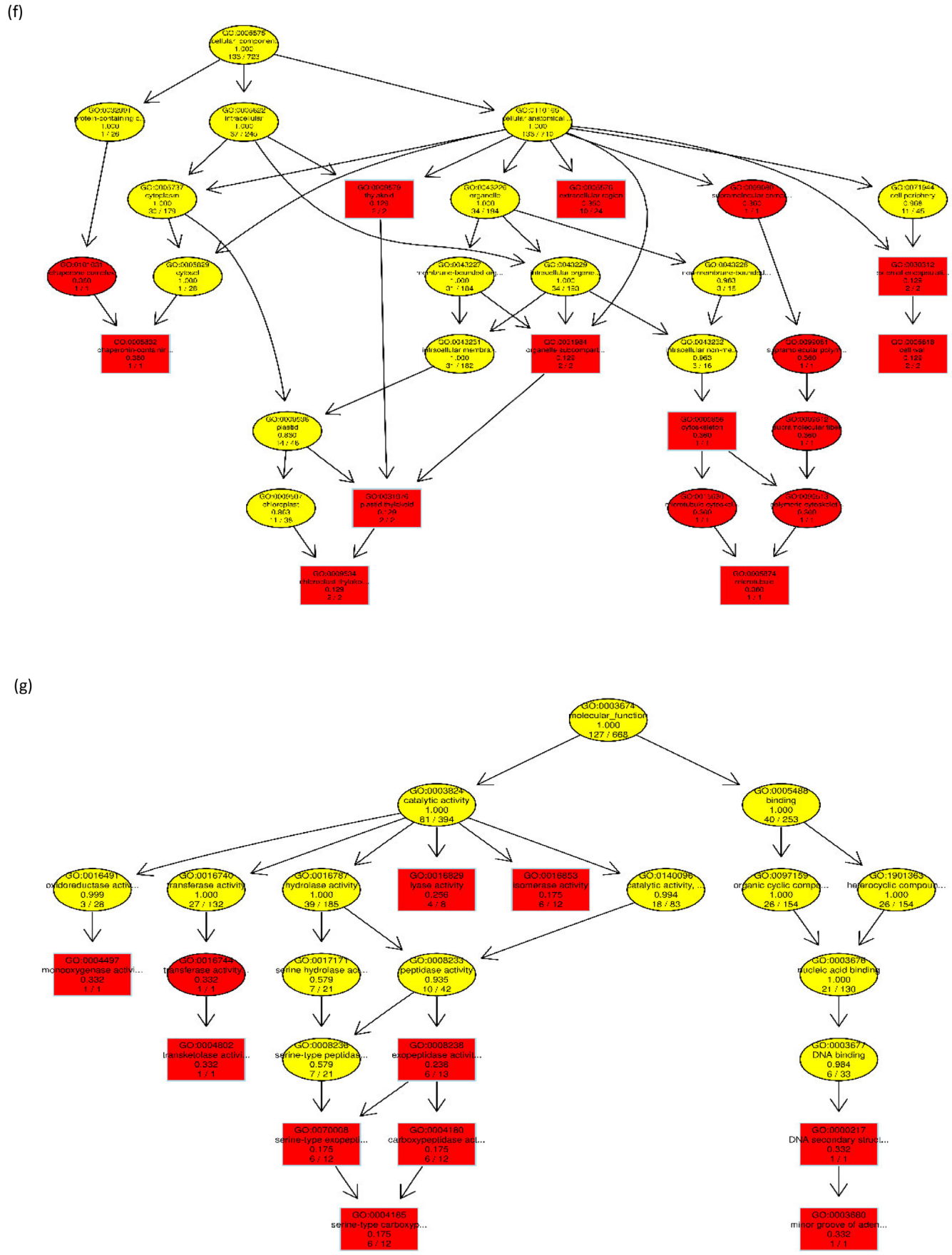

FIGURE 4 | (Continued)

(h)

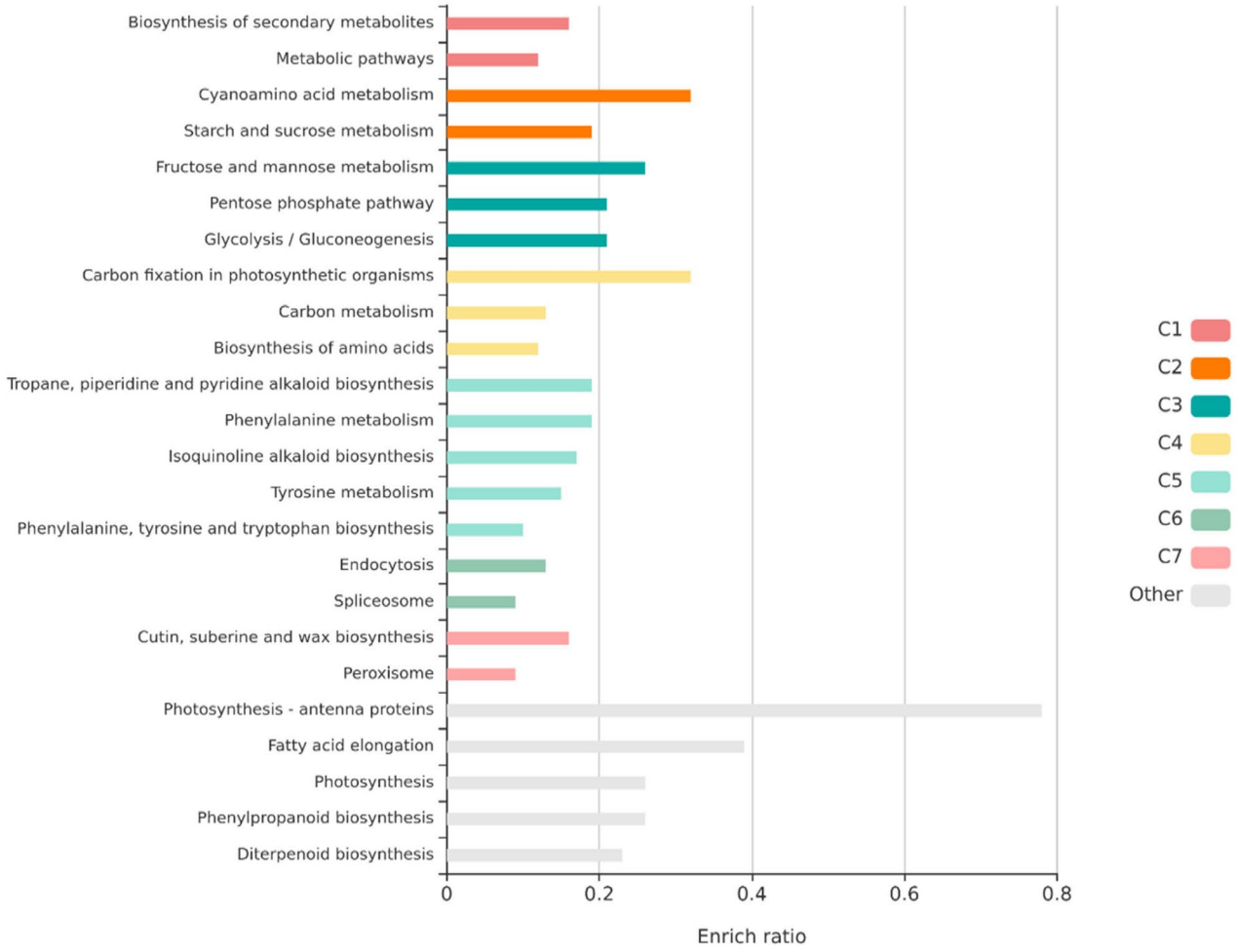

FIGURE 4 | (Continued)

TABLE 6 | Putative candidate genes identified through GWAS and RNA sequencing.

S. No.	Gene Id	Chromosome	Start position	End position	Protein/Functional homolog
1	Sobic.002G106200	Chr02	12693075	12695337	F-box domain-containing protein
	Sobic.005G077900	Chr05	9618086	9621970	F-box domain-containing protein
2	Sobic.003G216300	Chr03	55158214	55164924	ABC transporter G family member 40
	Sobic.007G095100	Chr07	17560153	17564153	ABC transporter domain-containing protein
3	Sobic.008G135800	Chr08	56450045	56452857	Lipase_GDSL domain-containing protein
4	Sobic.009G111200	Chr09	44785084	44786853	AP2/ERF domain-containing protein
5	Sobic.004G133500	Chr04	21147714	21152806	Bidirectional sugar transporter SWEET
6	Sobic.004G269900	Chr04	61416646	61421827	WRC domain-containing protein
7	Sobic.005G052500	Chr05	5292803	5295875	Aa_trans domain-containing protein
8	Sobic.006G048700	Chr06	34,559165	34562646	Acyl-[acyl-carrier-protein] desaturase
9	Sobic.007G098800	Chr07	20594640	20618760	Protein kinase domain superfamily protein
10	Sobic.007G101500	Chr07	25707028	25712978	Glucose-1-phosphate adenylyl transferase
11	Sobic.007G101800	Chr07	26843061	26848085	PFK domain-containing protein
12	Sobic.006G045400	Chr06	31848665	31851676	Amino acid selective channel protein

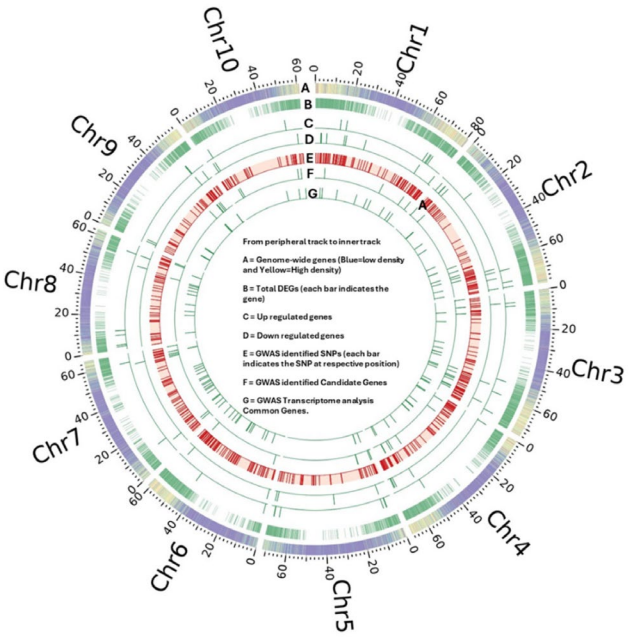

FIGURE 5 | CIRCOS plot depicting the comparative analysis of GWAS and Transcriptome analysis of the contrasting sorghum accessions. Plot to be read from peripheral track to inner track A = genome-wide genes (Blue = low density and Yellow = high density), B = total DEGs (each bar indicates the gene), C = up regulated genes, D = down regulated genes, E = GWAS identified SNPs (each bar indicates the SNP at respective position), F = GWAS identified Candidate Genes, and G = GWAS and Transcriptome analysis validated genes.

In summary, based on combined GWAS and transcriptomics analysis, we identified a total of 10 key candidate genes mapping to seven chromosomes (2, 3, 4, 5, 6, 7, and 9) of sorghum. These are as follows:

1. *Sobic.002G106200* (Chr 2): F-box protein; regulates nitrogen metabolism by mediating targeted degradation of nitrate and ammonium transporters.
2. *Sobic.003G216300* (Chr 3): ABC transporter; major role in nitrate and ammonium uptake and translocation.
3. *Sobic.004G269900* (Chr 4): NLP (NIN-like protein, WRC domain); master regulator of nitrogen signaling and assimilation.
4. *Sobic.004G133500* (Chr 4): Bi-directional sugar transporter (SWEET); links carbon and nitrogen metabolism and stress adaptation.
5. *Sobic.005G052500* (Chr 5): Amino acid–selective channel protein; facilitates ammonium and amino acid transport for nitrogen distribution.
6. *Sobic.006G045400* (Chr 6): Glutamine synthetase (GS); key enzyme for ammonium assimilation in nitrogen metabolism.
7. *Sobic.007G095100* (Chr 7): ABC transporter; involved in nitrogen uptake and stress adaptation.
8. *Sobic.007G101500* (Chr 7): Glucose-1-phosphate adenylyl transferase (AGPase) plays a pivotal role in carbon-nitrogen partitioning and yield.
9. *Sobic.007G101800* (Chr 7): Phosphofructokinase (PFK) plays an important role in glycolysis and nitrogen assimilation.
10. *Sobic.009G111200* (Chr 9): AP2/ERF transcription factor; orchestrates nitrate transporter gene regulation and nitrogen-responsive networks.

3.9 | Comparative Assessment of Homologous Genes Across Related Crop Species

Homologous gene groups across sorghum, rice, wheat, maize, pearl millet, and foxtail millet were identified using comparative assessment. This analysis provided significant insights into the homology among major cereal crops, highlighting evolutionary relationships and patterns of functional conservation. A detailed description of these gene functions and their homology with other cereals is presented in Table S5, Figure S1 and is further discussed in the integrative analysis of GWAS and transcriptome analysis section. This analysis uncovered 35 reciprocal best-matching gene pairs shared among sorghum, pearl millet, rice, foxtail millet, wheat, and maize, indicating robust genetic conservation across these species. These gene pairs likely represent core functional genes necessary for fundamental biological processes conserved across diverse cereal lineages. Furthermore, 38 orthologous gene pairs were conserved across sorghum, pearl millet, foxtail millet, wheat, and maize, highlighting the hypothesis of a common ancestral gene set among these cereals. Interestingly, two orthologous gene pairs exclusive to sorghum, foxtail millet, wheat, and maize indicate potential divergence patterns induced by species-specific adaptations. Notably, a single orthologous gene pair was detected among sorghum, foxtail millet, and pearl millet, which may reflect genetic relationships unique to the Panicoideae subfamily. In addition to shared gene pairs, 28 unique putative candidate genes were identified exclusively in sorghum, potentially demonstrating lineage-specific adaptations or unique functional attributes. These sorghum-specific genes offer promising targets for functional characterization, particularly in the context of stress tolerance, agronomic performance, and domestication traits. Overall, these findings enhance our understanding of genomic conservation and divergence among cereals, offering potential avenues for comparative genomics driven crop improvement.

4 | Conclusion

Improving NUE is critical to mitigate the economic and environmental challenges posed by N fertilizer-intensive cereal cropping systems globally. This is the first comprehensive report on sorghum on the N responsiveness across diverse sorghum accessions and the underlying key candidate genes. This pioneering study in sorghum investigated NUE and associated agronomic traits under varied N regimes and successfully identified a distinct set of contrasting sorghum accessions for

NUE. GWAS analysis pinpointed important genetic loci related to NUE and other relevant traits. Through genotype-specific N treatment and timepoint-oriented transcriptome analysis of contrasting sorghum accessions for N stress tolerance, we identified differentially expressed genes and gene networks linked to NUE and various abiotic stresses. A comparative analysis of GWAS and transcriptome datasets helped identify key candidate genes for NUE and other traits, showcasing significant potential in uncovering the genetic variation for NUE in sorghum. Analysis of identified homologous gene groups across major cereals revealed evolutionary relationships and genetic conservation. The comprehensive insights, genetic and genomic resources, and genetic markers from this study offer valuable support to researchers and breeders working on NUE improvement, enabling them to devise sustainable crop improvement programs. This exhaustive analysis not only uncovered key avenues for systematic dissection of NUE in sorghum but also paved the way for its potential translation into other cereal crops. The identified candidate genes may be used for further molecular dissection of NUE-related traits. These genes may be deployed using genomics-assisted breeding and could be attractive targets for gene editing.

5 | Material and Methods

5.1 | Plant Material and Experimental Design

A diverse panel of 186 sorghum accessions, comprising the sorghum reference set, promising breeding lines, and accessions from various countries with similar phenology, was used in this study (Table S1). Field experiments were conducted for two seasons (2017–18 and 2018–19) in black soil precision fields of the International Crops Research Institute for the Semi-Arid Tropics (ICRISAT), Hyderabad, Telangana, India. For both seasons, sorghum accessions were evaluated in a split-plot alpha lattice design (2017–18: 24 blocks × 8 plots and 2018–19: 27 blocks × 7 plots) with three replications under three N dosages (0%, 50%, and 100% of the recommended N (90 Kg ha^{-1})). Seeds were sown using a four-cone planter on raised furrows at 15–20 seeds per row. Each accession was grown in a four-row plot, two meters long, with 0.60 m row spacing and 0.15 m between plants. N fertilizer was applied to N50 and N100 plots as urea (46% N) in two splits. All plots received uniform applications of single super phosphate (16% P_2O_5, 50 kg ha^{-1}) and muriate of potash (60% K_2O, 40 kg ha^{-1}) in two splits (Bollam et al. 2021). Standard irrigation, pest, and disease management practices were followed to minimize yield loss throughout the crop period.

5.2 | Sampling and Measurement of Traits

Chlorophyll content (CC) was recorded on the flag leaf of three randomly selected plants from the middle two rows of each plot using a SPAD meter (Konica Minolta Sensing Americas Inc., Ramsey, NJ) at the anthesis stage (75 days post emergence). Days to 50% flowering (DFL), leaf area (LA), leaf number (LN), plant height (PH), number of tillers (NT), fresh and dry straw yield (FSY and DSY; g/plot), panicle number (PN), panicle weight (PW; g/plot), grain yield (GY; g/plot), test weight (TW; 200 seed weight in g) were recorded as described by Bollam et al. (2021). Grain N (GN) and straw N (SN) contents were estimated by the sulfuric acid-selenium digestion method (Sahrawat et al. 2002) with an auto-analyzer (Skalar SAN System, AA Breda, Netherlands).

5.3 | Genotyping-By-Sequencing and Single Nucleotide Polymorphism Calling

Leaf tissue from 12-day-old seedlings (4–6-leaf stage) of each accession was collected, and DNA was extracted using a modified CTAB protocol (Mace et al. 2003). DNA quality was verified on 0.8% agarose gel, and concentrations were quantified using a Nanodrop2000 (Thermo Scientific, USA). Genotyping was performed following the genotyping by sequencing (GbS) method (Elshire et al. 2011). DNA was digested with the *ApeKI* restriction enzyme, ligated to barcode adapters, pooled in equal quantities, and used for library construction. Libraries were sequenced on the Illumina HiSeq 2500 platform (Illumina Inc., San Diego, CA, United States), yielding ~489 million raw reads from 186 genotypes. For SNP calling, TASSEL v5.2 GBS pipeline (Bradbury et al. 2007) was used against reference sorghum genome assembly v3.1 (https://phytozome-next.jgi.doe.gov/info/Sbicolor_v3_1_1). Read quality was assessed using the Subre tool; low-quality and adapter-contaminated reads were removed, and barcode reads were further sorted and demultiplexed. A total of 22,439 high-quality SNPs with minor allele frequency (MAF) > 1% and < 50% missing data were retained for downstream genotyping analysis.

5.4 | Diversity and Population Structure

A phylogenetic tree was constructed using the unweighted neighbour-joining method in TASSEL v5.2 (TASSEL v5.2). Population structure of the 186 sorghum accessions was analysed in ADMIXTURE (Alexander et al. 2009) based on the maximum-likelihood method. Cross-validation (CV) was implemented across *K*-values ranging from 2 to 8, with 10-fold cross-validations employed to determine an optimal *K*-value, showing the lowest prediction error and consistent clustering with the hierarchical tree.

5.5 | Statistical Analysis

Analysis of variance (ANOVA) for all traits, both within and across seasons, was performed using the PROC MIXED procedure in SAS version 9.4 (SAS Institute Inc. 2018). Season, treatment (whole plot), genotype (subplot), and replications were treated as fixed effects, while block was considered a random effect. Individual season variances were modelled into the combined analysis. Best Linear Unbiased Estimates (BLUE's) were calculated for main and interaction effects of season, treatment, and genotype. Multiple comparisons were performed for significant effects ($p < 0.05$); correlation coefficient analysis was performed using the PROC CORR.

5.6 | Genome-Wide Association Studies (GWAS)

GWAS was performed for the panel by using the two seasons' phenotypic data (BLUEs) on different morpho-physiological and yield attributes (CC, DFL, LA, LN, NT, PH, PN, FSY, DSY, PW, TW, PHI) related to NUE, together with the genotypic data with a total of 22,439 high-quality SNPs, with minor allele frequency (MAF) > 1% and missing data < 50%. Missing genotypes were imputed using the Beagle v5.1 algorithm (Browning et al. 2018) implemented in TASSEL v5.0 (Bradbury et al. 2007) prior to GWAS analysis. GWAS was performed using Genomic Association and Prediction-Integrated Tool (GAPIT) in R (Lipka et al. 2012) using the Settlement of MLM Under the Progressively Exclusive Relationship (SUPER) model (Wang et al. 2014). For GWAS, population structure was statistically controlled by including the first three principal components (PC1–PC3) derived from genome-wide SNP data, which captured the major variance axes corresponding to these clusters. Relatedness among individuals was accounted for using a centered identity-by-state (IBS) kinship matrix. This PC + K mixed-model framework is widely used in crop GWAS to reduce false positives by correcting for both population stratification and cryptic relatedness (Price et al. 2006; Yu et al. 2006; Lipka et al. 2012). Marker–trait associations were considered significant at FDR < 0.05 (Benjamini and Hochberg 1995), and the distribution of marker *p*-values across the sorghum chromosomes was visualized as Manhattan plots using the position of chromosome as the *x*-axis and *p* value ($-\log^{10}$) as the *y*-axis.

5.7 | Identification of the Putative Candidate Genes

Significant SNPs showing marker-trait associations and in linkage disequilibrium (LD) with specific traits were used to identify putative candidate genes through the generic genome browser (GBrowse; Donlin 2009; Stein 2013). The identified genes were BLAST searched against the sorghum reference genome for functional annotations. Both known and novel genes involved in N stress tolerance and other abiotic stress mechanisms were identified.

5.8 | Screening of Contrasting Sorghum Accessions for RNA Sequencing

Seeds of contrasting sorghum lines (High NUE: ICSV745 and Low NUE: HDW703), selected from Bollam et al. (2021) and the present study, were germinated in sand. Eight-day-old seedlings with uniform growth (both plumule and radicle) were transferred to a hydroponic system containing nutrient media (Modified Hoagland) in glass house conditions (16/8 h photoperiod; 25°C (day) and 18°C (night), pH 5.8) (Figure 2a,b). The nutrient solution was refreshed every 3 days. Two-week-old seedlings were N starved for 2 days by replacing the medium with an N free solution, followed by exposure to two N levels (0% and 100% of the standard Hoagland N concentration). Shoot and root samples of plants from two N treatments were harvested separately (at 30 min and 6 h after N induction), flash frozen in liquid nitrogen, and stored at −80°C until RNA isolation. For each sample and treatment, three biological replicates were maintained.

5.9 | RNA Extraction From the Shoot and Root Samples

Total RNA was isolated from the collected shoot and root tissues [ICSV745_30m_N0_Shoot (1), ICSV745_30m_N0_Root (2), ICSV745_30m_N100_Shoot (3), ICSV745_30m_N100_Root (4), ICSV745_6h_N0_Shoot (5), ICSV745_6h_N0_Root (6), ICSV745_6h_N100_Shoot (7), ICSV745_6h_N100_Root (8), HDW703_30m_N0_Shoot (9), HDW703_30m_N0_Root (10), HDW703_30m_N100_Shoot (11), HDW703_30m_N100_Root (12), HDW703_6h_N0_Shoot (13), HDW703_6h_N0_Root (14), HDW703_6h_N100_Shoot (15), HDW703_6h_N100_Root (16)] of contrasting sorghum genotypes ICSV745 and HDW703 using the RNeasy Plant Mini kit (Qiagen, Germany) as per the manufacturer's instructions. RNA was treated with RNAse-free DNAse enzyme (Thermo Scientific, USA). RNA was eluted in nuclease-free water (Ambion, USA). The quantification and quality of the isolated RNA were assessed using Nanodrop2000 (Thermo Scientific, USA) and QubitTM Fluorometer (Thermo Scientific, USA) respectively. The integrity of RNA was determined by using Agilent 2100 Bioanalyzer (Agilent Technologies, USA).

5.10 | Library Preparation and Illumina Sequencing

Five hundred ng (500 ng) of total RNA was used for mRNA isolation, fragmentation and priming. Fragmented and primed mRNA was used to synthesize double-stranded complementary DNA (dscDNA). The dscDNA was purified using JetSeq Beads (Meridian Bioscience, USA). Purified dscDNA was end-repaired, adenylated, and ligated to Illumina multiplex barcode adapters as per NEBNext Ultra II Directional RNA Library Prep protocol followed by second strand excision using USER enzyme at 37°C for 15 min. Adapter ligated cDNA was purified using JetSeq Beads and was subjected to 11 cycles for Indexing- (98°C for 30 s, cycling) (98°C for 10 s, 65°C for 75 s) and 65°C for 5 min to enrich the adapter-ligated fragments. The final PCR product (sequencing library) was purified with JetSeq Beads, followed by a library quality control check. The generated cDNA library was quantified by Qubit Fluorometer (ThermoFisher Scientific, USA) and its fragment size distribution analyzed on Agilent 2200 TapeStation. The 16 cDNA libraries were sequenced using Illumina NovaSeq6000 (150 × 2 chemistry) (Illumina Inc., USA).

5.11 | RNA Sequencing Data Analysis

The raw RNASeq datasets were filtered to remove adaptors and low-quality bases using the Trimmomatic tool (Bolger et al. 2014), and the high-quality reads were mapped to the sorghum reference (v3.1) with the hisat2 tool (Kim et al. 2019). The read mapping was measured with featureCounts from subread-1.4.6 (Liao et al. 2013), and differentially expressed genes were identified with the R package "DESeq" (Wang et al. 2009). Genes with an absolute $\log_2$ fold-change ≥ 1 (≥ two-fold change in expression) and a false discovery rate (FDR) ≤ 0.05, adjusted using the Benjamini–Hochberg method, were considered significantly differentially expressed. Enrichment analysis was performed with the R package "topGO" (Alexa

and Rahnenfuhrer, 2016), "Rgraphviz" (Gentry et al. 2010), and KOBAS (Bu et al. 2021).

5.12 | Integrated GWAS and RNA-Seq Analysis for Candidate Gene Identification and Cross-Species Homology

The putative candidate genes identified through GWAS analysis were compared with RNA sequencing data. Comparative analysis was performed to align MTAs from GWAS with DEGs from RNA sequencing, identifying overlapping genes or genomic regions. Additionally, putative homologous gene groups across sorghum, rice, wheat, maize, pearl millet, and foxtail millet were identified using NCBI TBLASTX. Reciprocal best-match homologous gene pairs between sorghum and other related crop species were designated as putative orthologous gene pairs.

Author Contributions

Rajeev Gupta, Santosh P. Deshpande, and Rakesh K. Srivastava led the project, conceptualized, and designed the research strategy. Srikanth Bollam performed field, greenhouse, and lab experiments, analyzed and interpreted the data, wrote, and revised the manuscript. Kirandeep Kaur Romana and Laavanya Rayaprolu performed field and lab experiments, phenotyping, interpreted the data, and co-wrote the results section of the manuscript. Damaris A. Odeny, Abhishek Rathore, Pradeep Ruperao, Sivasubramani Selvanayagam, Gopikrishna Adapala, Vinod Kumar Valluri, and Prasad Bajaj carried out statistical and bioinformatics analysis. All authors contributed to writing the manuscript. Rakesh K. Srivastava revised and edited the manuscript for final publication.

Acknowledgements

Funding support was provided by the Department of Biotechnology (DBT), Government of India, the Biotechnology and Biological Sciences Research Council (BBSRC), United Kingdom, for the CINTRIN-1 (BT/IN/UK-VNC/42/RG/2015-16 and BB/N013441/1) and CINTRIN-2 (BT/PR42631/AGIII/103/1312/2021) projects to Rajeev Gupta, Rakesh K. Srivastava, Santosh P. Deshpande, Abhishek Rathore, Laavanya Rayaprolu, Kirandeep Kaur Romana. The Department of Science and Technology–National Science and Engineering Research Board (DST-SERB) (PDF/2016/003203) provided support for the National Post-Doctoral Fellowship (NPDF) to Srikanth Bollam. This work was published as part of the CGIAR Research Program on Grain Legumes and Dryland Cereals (CRP-GLDC).

Funding

This work was supported by the Department of Biotechnology (DBT), Ministry of Science and Technology, Government of India, BT/IN/UK-VNC/42/RG/2015-16, BT/PR42631/AGIII/103/1312/2021. Biotechnology and Biological Sciences Research Council, BB/N013441/1. Department of Science and Technology–National–Science and Engineering Research Board (DST–SERB), PDF/2016/003203. CGIAR Research Program on Grain Legumes and Dryland Cereals.

Ethics Statement

The authors have nothing to report.

Conflicts of Interest

The authors declare no conflicts of interest.

Data Availability Statement

The transcriptome sequencing data generated in this study have been deposited in the NCBI Sequence Read Archive (SRA) under the BioProject ID: PRJNA1321159, with BioSample IDs: SAMN51201369 to SAMN51201384, and SRA Accession Numbers: SRR35509016 to SRR35509031. Additionally, the genotypic and phenotypic datasets used in the study have been deposited in the Dataverse repository and can be accessed with the following DOIs: Genotypic data—https://doi.org/10.21421/D2/DU8VOI; Phenotypic data—https://doi.org/10.21421/D2/XTDY2R.

References

Achakzai, A. K. K., B. H. S. Habibullah, and M. A. Wahid. 2012. "Effect of Nitrogen Fertilizer on the Growth of Mungbean [*Vigna radiata* (L.) Wilczek] Grown in Quetta." *Pakistan Journal of Botany* 44, no. 3: 981–987.

Afolayan, G., S. P. Deshpande, S. E. Aladele, et al. 2019. "Genetic Diversity Assessment of Sorghum (*Sorghum bicolor* (L.) Moench) Accessions Using Single Nucleotide Polymorphism Markers." *Plant Genetic Resources: Characterization and Utilization* 17, no. 5: 412–420.

Ajeigbe, H. A., F. M. Akinseye, K. Ayuba, and J. Jonah. 2018. "Productivity and Water Use Efficiency of Sorghum [*Sorghum bicolor* (L.) Moench] Grown Under Different Nitrogen Applications in Sudan Savanna Zone, Nigeria." *International Journal of Agronomy* 2018: 7676058.

Al Salameen, F., N. Habibi, S. Uddin, et al. 2020. "Spatio-Temporal Variations in Bacterial and Fungal Community Associated With Dust Aerosol in Kuwait." *PLoS One* 15, no. 11: e0241283.

Alexa, A., and J. Rahnenführer. 2009. "Gene Set Enrichment Analysis With topGO." *Bioconductor Improv* 27: 1–26.

Alexander, D. H., J. Novembre, and K. Lange. 2009. "Fast Model-Based Estimation of Ancestry in Unrelated Individuals." *Genome Research* 19, no. 9: 1655–1664.

Ali, A. E. E. 2019. "Comparative Molecular, Physiological and Proteomic Analyses of Maize and Sorghum Subjected to Water Deficit Stress (Doctoral Dissertation)."

Alomari, D. Z., A. M. Alqudah, K. Pillen, N. von Wirén, and M. S. Röder. 2021. "Toward Identification of a Putative Candidate Gene for Nutrient Mineral Accumulation in Wheat Grains for Human Nutrition Purposes." *Journal of Experimental Botany* 72, no. 18: 6305–6318.

Alvarez, J. M., E. Riveras, E. A. Vidal, D. E. Gras, O. Contreras-Lopez, and R. A. Gutiérrez. 2014. "Systems Approach Identifies TGA1 and TGA4 Transcription Factors as Important Regulators of Nitrate-deficiency Responses in Arabidopsis." *Plant Cell* 26, no. 5: 1971–1984. https://doi.org/10.1105/tpc.114.124187.

Anil Kumar, S., P. Hima Kumari, M. Nagaraju, et al. 2022. "Genome-Wide Identification and Multiple Abiotic Stress Transcript Profiling of Potassium Transport Gene Homologs in *Sorghum bicolor*." *Frontiers in Plant Science* 13: 3088.

Anur, R. M., N. Mufithah, W. D. Sawitri, H. Sakakibara, and B. Sugiharto. 2020. "Overexpression of Sucrose Phosphate Synthase Enhanced Sucrose Content and Biomass Production in Transgenic Sugarcane." *Plants* 9, no. 2: 200.

Bandyopadhyay, T., S. M. Swarbreck, V. Jaiswal, et al. 2022. "GWAS Identifies Genetic Loci Underlying Nitrogen Responsiveness in the Climate Resilient C4 Model *Setaria italica* (L.)." *Journal of Advanced Research* 42: 249–261.

Belete, F., N. Dechassa, A. Molla, and T. Tana. 2018. "Effect of Nitrogen Fertilizer Rates on Grain Yield and Nitrogen Uptake and Use Efficiency of Bread Wheat (*Triticum aestivum* L.) Varieties on the Vertisols of Central Highlands of Ethiopia." *Agriculture & Food Security* 7, no. 1: 1–12.

Benjamini, Y., and Y. Hochberg. 1995. "Controlling the False Discovery Rate: A Practical and Powerful Approach to Multiple Testing." *J R Stat Soc Series B* 57, no. 1: 289–300.

Boatwright, J. L., S. Sapkota, M. Myers, et al. 2022. "Dissecting the Genetic Architecture of Carbon Partitioning in Sorghum Using Multiscale Phenotypes." *Frontiers in Plant Science* 13: 790005.

Bolger, A. M., M. Lohse, and B. Usadel. 2014. "Trimmomatic: A Flexible Trimmer for Illumina Sequence Data." *Bioinformatics* 30, no. 15: 2114–2120.

Bollam, S., K. K. Romana, L. Rayaprolu, et al. 2021. "Nitrogen Use Efficiency in Sorghum: Exploring Native Variability for Traits Under Variable N-Regimes." *Frontiers in Plant Science* 12: 643192.

Bradbury, P. J., Z. Zhang, D. E. Kroon, T. M. Casstevens, Y. Ramdoss, and E. S. Buckler. 2007. "TASSEL: Software for Association Mapping of Complex Traits in Diverse Samples." *Bioinformatics* 23, no. 19: 2633–2635.

Browning, B. L., Y. Zhou, and S. R. Browning. 2018. "A One-Penny Imputed Genome from Next-Generation Reference Panels." *American Journal of Human Genetics* 103, no. 3: 338–348. https://doi.org/10.1016/j.ajhg.2018.07.015.

Bu, D., H. Luo, P. Huo, et al. 2021. "KOBAS-i: Intelligent Prioritization and Exploratory Visualization of Biological Functions for Gene Enrichment Analysis." *Nucleic Acids Research* 49, no. W1: W317–W325.

Busta, L., E. Schmitz, D. K. Kosma, J. C. Schnable, and E. B. Cahoon. 2021. "A Co-Opted Steroid Synthesis Gene, Maintained in Sorghum but Not Maize, Is Associated With a Divergence in Leaf Wax Chemistry." *Proceedings of the National Academy of Sciences of the United States of America* 118, no. 12: e2022982118.

Cai, H., Y. Lu, W. Xie, T. Zhu, and X. Lian. 2012. "Transcriptome Response to Nitrogen Starvation in Rice." *Journal of Biosciences* 37: 731–747.

Calabrese, S. 2016. "Nutrient Transport in the Arbuscular Mycorrhizal Symbiosis: The Regulation of Nutrient Transporters in Rhizophagus Irregularis and Its Host Plants Populus Trichocarpa and *Sorghum bicolor* (Doctoral Dissertation, University_of_Basel)."

Cao, S., Y. Wang, X. Li, F. Gao, J. Feng, and Y. Zhou. 2020. "Characterization of the AP2/ERF Transcription Factor Family and Expression Profiling of DREB Subfamily Under Cold and Osmotic Stresses in Ammopiptanthus Nanus." *Plants (Basel)* 9, no. 4: 455.

Chen, X., Y. Ding, Y. Yang, et al. 2021. "Protein Kinases in Plant Responses to Drought, Salt, and Cold Stress." *Journal of Integrative Plant Biology* 63, no. 1: 53–78.

Cheng, Z., X. Zhang, W. Yao, et al. 2021. "Genome-Wide Identification and Expression Analysis of the Xyloglucan Endotransglucosylase/Hydrolase Gene Family in Poplar." *BMC Genomics* 22: 1–13.

Ciampitti, I. A., and P. V. V. Prasad. 2021. "Nitrogen Management in Sorghum." *Frontiers in Plant Science* 12: 643623.

Cohen, D., M. B. Bogeat-Triboulot, E. Tisserant, et al. 2010. "Comparative Transcriptomics of Drought Responses in Populus: A Meta-Analysis of Genome-Wide Expression Profiling in Mature Leaves and Root Apices Across Two Genotypes." *BMC Genomics* 11: 1–21.

Denancé, N., B. Szurek, and L. D. Noël. 2014. "Emerging Functions of Nodulin-Like Proteins in Non-Nodulating Plant Species." *Plant and Cell Physiology* 55, no. 3: 469–474.

Diao, J., S. Li, L. Ma, et al. 2021. "Genome-Wide Analysis of Major Facilitator Superfamily and Its Expression in Response of Poplar to Fusarium Oxysporum." *Frontiers in Genetics* 12: 769888.

Do, T. H. T., E. Martinoia, Y. Lee, and J. U. Hwang. 2021. "2021 Update on ATP-Binding Cassette (ABC) Transporters: How They Meet the Needs of Plants." *Plant Physiology* 187, no. 4: 1876–1892.

Donlin, M. J. 2009. "Using the Generic Genome Browser (GBrowse)." *Current Protocols in Bioinformatics* 28, no. 1: 9.

Dossou-Aminon, I., L. Y. Loko, A. Adjatin, et al. 2015. "Genetic Divergence in Northern Benin Sorghum (*Sorghum bicolor* L. Moench) Landraces as Revealed by Agromorphological Traits and Selection of Candidate Genotypes." *TheScientificWorldJOURNAL* 2015: 916476.

Drobnitch, S. T., L. H. Comas, N. Flynn, et al. 2021. "Drought-Induced Root Pressure in *Sorghum bicolor*." *Frontiers in Plant Science* 12: 571072.

Elshire, R. J., J. C. Glaubitz, Q. Sun, et al. 2011. "A Robust, Simple Genotyping-By-Sequencing (GBS) Approach for High Diversity Species." *PLoS One* 6, no. 5: e19379.

Erisman, J. W., M. A. Sutton, J. Galloway, Z. Klimont, and W. Winiwarter. 2008. "How a Century of Ammonia Synthesis Changed the World." *Nature Geoscience* 1: 636–639.

Feng, H., X. Fan, M. Yan, X. Liu, A. J. Miller, and G. Xu. 2011. "Multiple Roles of Nitrate Transport Accessory Protein NAR2 in Plants." *Plant Signaling & Behavior* 6, no. 9: 1286–1289.

Fernie, A. R., C. W. Bachem, Y. Helariutta, et al. 2020. "Synchronization of Developmental, Molecular and Metabolic Aspects of Source–Sink Interactions." *Nature Plants* 6, no. 2: 55–66.

Frink, C. R., P. E. Waggoner, and J. H. Ausubel. 1999. "Nitrogen Fertilizer: Retrospect and Prospect." *Proceedings of the National Academy of Sciences* 96, no. 4: 1175–1180.

Galloway, J. N., A. R. Townsend, J. W. Erisman, et al. 2008. "Transformation of the Nitrogen Cycle: Recent Trends, Questions, and Potential Solutions." *Science* 320, no. 5878: 889–892.

Garnett, T., D. Plett, V. Conn, et al. 2015. "Variation for N uptake Systems in Maize: Genotypic, Developmental, and Nitrogen Condition Effects." *Plant Physiology* 167, no. 2: 1111–1127. https://doi.org/10.1104/pp.114.257819.

Geigenberger, P. 2011. "Regulation of Starch Biosynthesis in Response to a Fluctuating Environment: Implications for Yield and Biomass Production." *Plant Physiology* 155, no. 1: 13–28. https://doi.org/10.1104/pp.110.165854.

Geldner, N., J. Friml, Y. D. Stierhof, G. Jürgens, and K. Palme. 2001. "Auxin Transport Inhibitors Block PIN1 Cycling and Vesicle Trafficking." *Nature* 413, no. 6854: 425–428.

Gelli, M., Y. Duo, A. R. Konda, C. Zhang, D. Holding, and I. Dweikat. 2014. "Identification of Differentially Expressed Genes Between Sorghum Genotypes With Contrasting Nitrogen Stress Tolerance by Genome-Wide Transcriptional Profiling." *BMC Genomics* 15: 1–16.

Gelli, M., A. R. Konda, K. Liu, et al. 2017. "Validation of QTL Mapping and Transcriptome Profiling for Identification of Candidate Genes Associated With Nitrogen Stress Tolerance in Sorghum." *BMC Plant Biology* 17, no. 1: 1–18.

Gelli, M., S. E. Mitchell, K. Liu, et al. 2016. "Mapping QTLs and Association of Differentially Expressed Gene Transcripts for Multiple Agronomic Traits Under Different Nitrogen Levels in Sorghum." *BMC Plant Biology* 16: 1–18.

Gentry, J., L. Long, R. Gentleman, et al. 2010. "Rgraphviz: Provides Plotting Capabilities for R Graph Objects, r Package Version 1.24.0."

Good, A. G., A. K. Shrawat, and D. G. Muench. 2004. "Can Less Yield More? Is Reducing Nutrient Input Into the Environment Compatible With Maintaining Crop Production?" *Trends in Plant Science* 9, no. 12: 597–605.

Guskov, A., N. Nordin, A. Reynaud, et al. 2012. "Structural Insights Into the Mechanisms of Mg^{2+} Uptake, Transport, and Gating by CorA." *Proceedings of the National Academy of Sciences* 109, no. 45: 18459–18464.

Guttieri, M. J., K. Frels, T. Regassa, B. M. Waters, and P. S. Baenziger. 2017. "Variation for Nitrogen Use Efficiency Traits in Current and Historical Great Plains Hard Winter Wheat." *Euphytica* 213, no. 4: 1–18.

Han, G., C. Lu, J. Guo, et al. 2020. "C2H2 Zinc Finger Proteins: Master Regulators of Abiotic Stress Responses in Plants." *Frontiers in Plant Science* 11: 115.

Hansen, C. C., D. R. Nelson, B. L. Møller, and D. Werck-Reichhart. 2021. "Plant Cytochrome P450 Plasticity and Evolution." *Molecular Plant* 14, no. 8: 1244–1265.

Hao, D. C., G. Ge, P. Xiao, Y. Zhang, and L. Yang. 2011. "The First Insight Into the Tissue Specific Taxus Transcriptome via Illumina Second Generation Sequencing." *PLoS One* 6, no. 6: e21220.

He, L., J. M. Chen, H. Croft, et al. 2017. "Nitrogen Availability Dampens the Positive Impacts of CO2 Fertilization on Terrestrial Ecosystem Carbon and Water Cycles." *Geophysical Research Letters* 44, no. 22: 11–590.

Hirel, B., F. Chardon, and J. Durand. 2007. "The Contribution of Molecular Physiology to the Improvement of Nitrogen Use Efficiency in Crops." *Journal of Crop Science and Biotechnology* 10, no. 3: 123–132.

Hirel, B., J. Le Gouis, B. Ney, and A. Gallais. 2007. "The Challenge of Improving Nitrogen Use Efficiency in Crop Plants: Towards a More Central Role for Genetic Variability and Quantitative Genetics Within Integrated Approaches." *Journal of Experimental Botany* 58, no. 9: 2369–2387.

Huang, W., Y. He, L. Yang, et al. 2021. "Genome-Wide Analysis of Growth-Regulating Factors (GRFs) in *Triticum aestivum*." *PeerJ* 9: e10701.

Huh, S. U. 2021. "The Role of Pumilio Rna Binding Protein in Plants." *Biomolecules* 11, no. 12: 1851.

Isin, E. M., and F. P. Guengerich. 2007. "Complex Reactions Catalyzed by Cytochrome P450 Enzymes." *Biochimica et Biophysica Acta (BBA)-General Subjects* 1770, no. 3: 314–329.

Jiao, Y., Y. Wang, D. Xue, et al. 2010. "Regulation of OsSPL14 by OsmiR156 Defines Ideal Plant Architecture in Rice." *Nature Genetics* 42, no. 6: 541–544.

Jie, G. U. O., X. T. Zhou, K. L. Dai, et al. 2022. "Comprehensive Analysis of YABBY Gene Family in Foxtail Millet (*Setaria italica*) and Functional Characterization of SiDL." *Journal of Integrative Agriculture* 21, no. 10: 2876–2887.

Johnson, S. M., F. L. Lim, A. Finkler, H. Fromm, A. R. Slabas, and M. R. Knight. 2014. "Transcriptomic Analysis of *Sorghum Bicolor* Responding to Combined Heat and Drought Stress." *BMC Genomics* 15, no. 1: 1–19.

Kakumanu, A., M. M. Ambavaram, C. Klumas, et al. 2012. "Effects of Drought on Gene Expression in Maize Reproductive and Leaf Meristem Tissue Revealed by RNA-Seq." *Plant Physiology* 160, no. 2: 846–867.

Kanfany, G., R. El-Namaky, K. Ndiaye, K. Traore, and R. Ortiz. 2014. "Assessment of Rice Inbred Lines and Hybrids Under Low Fertilizer Levels in Senegal." *Sustainability* 6, no. 3: 1153–1162.

Kawasaki, T., H. Koita, T. Nakatsubo, et al. 2006. "Cinnamoyl-CoA Reductase, a Key Enzyme in Lignin Biosynthesis, Is an Effector of Small GTPase Rac in Defense Signaling in Rice." *Proceedings of the National Academy of Sciences* 103, no. 1: 230–235.

Kianifariz, M. 2017. "Transcriptome Analysis During Stem Development and in the a1 Cytoplasmic Male Sterility System of Sorghum (Doctoral Dissertation)."

Kim, D., J. M. Paggi, C. Park, C. Bennett, and S. L. Salzberg. 2019. "Graph-Based Genome Alignment and Genotyping With HISAT2 and HISAT-Genotype." *Nature Biotechnology* 37, no. 8: 907–915.

Konishi, M., and S. Yanagisawa. 2013. "Emergence of a New Step Towards Understanding the Regulation of Nitrate-responsive Gene Networks in Plants." *Plant & Cell Physiology* 54, no. 3: 351–357. https://doi.org/10.1093/pcp/pct003.

Krapp, A., R. Berthomé, M. Orsel, et al. 2011. "Arabidopsis Roots and Shoots Show Distinct Temporal Adaptation Patterns Toward Nitrogen Starvation." *Plant Physiology* 157, no. 3: 1255–1282.

Krill, A. M., M. Kirst, L. V. Kochian, E. S. Buckler, and O. A. Hoekenga. 2010. "Association and Linkage Analysis of Aluminum Tolerance Genes in Maize." *PLoS One* 5, no. 4: e9958.

Kryukov, A. A., A. O. Gorbunova, T. R. Kudriashova, et al. 2021. "Sugar Transporters of the SWEET Family and Their Role in Arbuscular Mycorrhiza." *Vavilov Journal of Genetics and Breeding* 25, no. 7: 754–760.

Kumar, M., V. Goyal, A. Shankar, A. Singh, D. K. Sahoo, and G. K. Pandey. 2022. "Genome-wide Analysis and Expression Profiling of Potassium Transport-related Genes in Rice under Drought and Salt Stress." *Physiologia Plantarum* 174, no. 1: e13632. https://doi.org/10.1111/ppl.13632.

Laperche, A., F. Devienne-Barret, O. Maury, J. Le Gouis, and B. Ney. 2006. "A Simplified Conceptual Model of Carbon/Nitrogen Functioning for QTL Analysis of Winter Wheat Adaptation to Nitrogen Deficiency." *Theoretical and Applied Genetics* 113, no. 6: 1131–1146.

Li, F., T. Asami, X. Wu, E. W. Tsang, and A. J. Cutler. 2007. "A Putative Hydroxysteroid Dehydrogenase Involved in Regulating Plant Growth and Development." *Plant Physiology* 145, no. 1: 87–97.

Li, X., W. Yan, H. Agrama, et al. 2012. "Unraveling the Complex Trait of Harvest Index With Association Mapping in Rice (*Oryza sativa* L.)." *PLoS One* 7, no. 1: e29350.

Liao, Y., G. K. Smyth, and W. Shi. 2013. "The Subread Aligner: Fast, Accurate and Scalable Read Mapping by Seed-And-Vote." *Nucleic Acids Research* 41, no. 10: e108.

Lipka, A. E., F. Tian, Q. Wang, et al. 2012. "GAPIT: Genome Association and Prediction Integrated Tool." *Bioinformatics* 28, no. 18: 2397–2399.

Liu, Y., Q. Song, D. Li, X. Yang, and D. Li. 2017. "Multifunctional Roles of Plant Dehydrins in Response to Environmental Stresses." *Frontiers in Plant Science* 8: 1018.

Luo, L., W. Li, K. Miura, M. Ashikari, and J. Kyozuka. 2012. "Control of Tiller Growth of Rice by OsSPL14 and Strigolactones, Which Work in Two Independent Pathways." *Plant and Cell Physiology* 53, no. 10: 1793–1801.

Mace, E. S., K. K. Buhariwalla, H. K. Buhariwalla, and J. H. Crouch. 2003. "A High-Throughput DNA Extraction Protocol for Tropical Molecular Breeding Programs." *Plant Molecular Biology Reporter* 21: 459–460.

Masclaux-Daubresse, C., F. Daniel-Vedele, J. Dechorgnat, et al. 2010. "Nitrogen Uptake, Assimilation, and Remobilization in Plants." *Journal of Experimental Botany* 61, no. 6: 1455–1467.

Maurel, C., Y. Boursiac, D. T. Luu, V. Santoni, Z. Shahzad, and L. Verdoucq. 2015. "Aquaporins in Plants." *Physiological Reviews* 95, no. 4: 1321–1358.

Meijón, M., S. B. Satbhai, T. Tsuchimatsu, and W. Busch. 2014. "Genome-Wide Association Study Using Cellular Traits Identifies a New Regulator of Root Development in Arabidopsis." *Nature Genetics* 46, no. 1: 77–81.

Meng, X., X. Wang, Z. Zhang, et al. 2021. "Transcriptomic, Proteomic, and Physiological Studies Reveal Key Players in Wheat Nitrogen Use Efficiency Under Both High and Low Nitrogen Supply." *Journal of Experimental Botany* 72, no. 12: 4435–4456.

Mizuno, D., K. Higuchi, T. Sakamoto, H. Nakanishi, S. Mori, and N. K. Nishizawa. 2003. "Three Nicotianamine Synthase Genes Isolated From Maize Are Differentially Regulated by Iron Nutritional Status." *Plant Physiology* 132, no. 4: 1989–1997.

Monostori, I., F. Szira, A. Tondelli, et al. 2017. "Genome-Wide Association Study and Genetic Diversity Analysis on Nitrogen Use

Efficiency in a Central European Winter Wheat (*Triticum aestivum* L.) Collection." *PLoS One* 12, no. 12: e0189265.

Morant, M., S. Bak, B. L. Møller, and D. Werck-Reichhart. 2003. "Plant Cytochromes P450: Tools for Pharmacology, Plant Protection and Phytoremediation." *Current Opinion in Biotechnology* 14, no. 2: 151–162.

Morris, G. P., P. Ramu, S. P. Deshpande, et al. 2013. "Population Genomic and Genome-Wide Association Studies of Agroclimatic Traits in Sorghum." *Proceedings of the National Academy of Sciences* 110, no. 2: 453–458.

Mudgil, Y., J. F. Uhrig, J. Zhou, B. Temple, K. Jiang, and A. M. Jones. 2009. "Arabidopsis N-MYC DOWNREGULATED-LIKE1, a Positive Regulator of Auxin Transport in a G Protein–Mediated Pathway." *Plant Cell* 21, no. 11: 3591–3609.

Mulaudzi-Masuku, T., R. D. Mutepe, O. C. Mukhoro, A. Faro, and B. Ndimba. 2015. "Identification and Characterization of a Heat-Inducible Hsp70 Gene From S Orghum Bicolor Which Confers Tolerance to Thermal Stress." *Cell Stress & Chaperones* 20: 793–804.

Muszynski, M. G., T. Dam, B. Li, et al. 2006. "Delayed flowering1 Encodes a Basic Leucine Zipper Protein That Mediates Floral Inductive Signals at the Shoot Apex in Maize." *Plant Physiology* 142, no. 4: 1523–1536.

Ng, A., and R. J. Xavier. 2011. "Leucine-Rich Repeat (LRR) Proteins: Integrators of Pattern Recognition and Signaling in Immunity." *Autophagy* 7, no. 9: 1082–1084.

Pan, H., Y. Shao, P. Yan, et al. 2016. "Reversible Aqueous Zinc/Manganese Oxide Energy Storage From Conversion Reactions." *Nature Energy* 1, no. 5: 1–7.

Paterson, A. H., J. E. Bowers, R. Bruggmann, et al. 2009. "The *Sorghum Bicolor* Genome and the Diversification of Grasses." *Nature* 457, no. 7229: 551–556.

Paterson, A. H., J. E. Bowers, and F. A. Feltus. 2008. "Genomics of Sorghum, a Semi-Arid Cereal and Emerging Model for Tropical Grass Genomics." In *Genomics of Tropical Crop Plants*, 469–482. Springer.

Preiss, J. 2009. "Biochemistry, Molecular Biology and Regulation of ADP-glucose Pyrophosphorylase in Plants." In *Biotechnology in Agriculture and Forestry: Transgenic Crop Plants*, 83–104. Springer.

Price, A. L., N. J. Patterson, R. M. Plenge, M. E. Weinblatt, N. A. Shadick, and D. Reich. 2006. "Principal Components Analysis Corrects for Stratification in Genome-Wide Association Studies." *Nature Genetics* 38, no. 8: 904–909. https://doi.org/10.1038/ng1847.

Pritchard, J. K., M. Stephens, and P. Donnelly. 2000. "Inference of Population Structure Using Multilocus Genotype Data." *Genetics* 155, no. 2: 945–959.

Pujarula, V., M. Pusuluri, S. Bollam, et al. 2021. "Genetic Variation for Nitrogen Use Efficiency Traits in Global Diversity Panel and Parents of Mapping Populations in Pearl Millet." *Frontiers in Plant Science* 12: 625915.

Quan, X., J. Zeng, L. Ye, et al. 2016. "Transcriptome Profiling Analysis for Two Tibetan Wild Barley Genotypes in Responses to Low Nitrogen." *BMC Plant Biology* 16, no. 1: 1–16.

Rao, I. S., C. N. Neeraja, B. Srikanth, et al. 2018. "Identification of Rice Landraces With Promising Yield and the Associated Genomic Regions Under Low Nitrogen." *Scientific Reports* 8, no. 1: 9200.

Raun, W. R., and G. V. Johnson. 1999. "Improving Nitrogen Use Efficiency for Cereal Production." *Agronomy Journal* 91, no. 3: 357–363.

Russo, V. M., L. C. Marett, M. M. Wright, M. J. Auldist, and W. J. Wales. 2017. "Whole-Tract Digestibility and Nitrogen-Use Efficiency of Partial Mixed Rations With and Without Canola Meal." *Animal Production Science* 57, no. 7: 1398–1404.

Sahrawat, K. L., G. R. Kumar, and K. V. S. Murthy. 2002. "Sulfuric Acid–Selenium Digestion for Multi-Element Analysis in a Single Plant Digest." *Communications in Soil Science and Plant Analysis* 33, no. 19–20: 3757–3765.

SAS Institute Inc. SAS® 9.4 Statements: Reference. 2018. *Version 5*. 3rd ed. SAS Institute Inc.

Satish, L., J. Shilpha, S. Pandian, et al. 2016. "Analysis of Genetic Variation in Sorghum (*Sorghum bicolor* (L.) Moench) Genotypes With Various Agronomical Traits Using SPAR Methods." *Gene* 576, no. 1: 581–585.

Shamme, S. K., C. V. Raghavaiah, T. Balemi, and I. Hamza. 2016. "Sorghum Growth, Productivity, Nitrogen Removal, N-Use Efficiencies and Economics in Relation to Genotypes and Nitrogen Nutrition in Kellem-Wollega Zone of Ethiopia, East Africa." *Advances in Crop Science and Technology* 4: 218–226.

Silva, T. N., J. B. Thomas, J. Dahlberg, and S. Y. Rhee. 2022. "Progress and Challenges in Sorghum Biotechnology, a Multipurpose Feedstock for the Bioeconomy." *Journal of Experimental Botany* 73, no. 3: 646–664. https://doi.org/10.1093/jxb/erab450.

Sinebo, W., R. Gretzmacher, and A. Edelbauer. 2004. "Genotypic Variation for Nitrogen Use Efficiency in Ethiopian Barley." *Field Crops Research* 85, no. 1: 43–60.

Singh, D., and A. Laxmi. 2015. "Transcriptional Regulation of Drought Response: A Tortuous Network of Transcriptional Factors." *Frontiers in Plant Science* 6: 895.

Singh, S. P., T. Pandey, R. Srivastava, et al. 2010. "BECLIN1 From *Arabidopsis thaliana* Under the Generic Control of Regulated Expression Systems, a Strategy for Developing Male Sterile Plants." *Plant Biotechnology Journal* 8, no. 9: 1005–1022.

Srikanth, B., I. S. Rao, K. Surekha, D. Subrahmanyam, S. R. Voleti, and C. N. Neeraja. 2016. "Enhanced Expression of OsSPL14 Gene and Its Association With Yield Components in Rice (*Oryza sativa*) Under Low Nitrogen Conditions." *Gene* 576, no. 1: 441–450.

Stein, L. D. 2013. "Using GBrowse 2.0 to Visualize and Share Next-Generation Sequence Data." *Briefings in Bioinformatics* 14, no. 2: 162–171.

Sui, B., X. Feng, G. Tian, X. Hu, Q. Shen, and S. Guo. 2013. "Optimizing Nitrogen Supply Increases Rice Yield and Nitrogen Use Efficiency by Regulating Yield Formation Factors." *Field Crops Research* 150: 99–107.

Swarup, R., and R. Bhosale. 2019. "Developmental Roles of AUX1/LAX Auxin Influx Carriers in Plants." *Frontiers in Plant Science* 10: 1306.

Tai, H., X. Lu, N. Opitz, et al. 2016. "Transcriptomic and Anatomical Complexity of Primary, Seminal, and Crown Roots Highlight Root Type-Specific Functional Diversity in Maize (*Zea mays* L.)." *Journal of Experimental Botany* 67, no. 4: 1123–1135.

Tegeder, M., and U. Z. Hammes. 2018. "The Way out and in: Phloem Loading and Unloading of Amino Acids." *Current Opinion in Plant Biology* 43: 16–21.

Tetlow, I. J., and M. J. Emes. 2017. "Starch Biosynthesis in the Developing Endosperms of Grasses and Cereals." *Agronomy* 7, no. 4: 81.

Wang, H., P. Zhao, X. Shen, et al. 2021. "Genome-Wide Survey of the Phosphofructokinase Family in Cassava and Functional Characterization in Response to Oxygen-Deficient Stress." *BMC Plant Biology* 21: 1–15.

Wang, Q., F. Tian, Y. Pan, E. S. Buckler, and Z. Zhang. 2014. "A SUPER Powerful Method for Genome Wide Association Study." *PLoS One* 9, no. 9: e107684.

Wang, X., G. Yang, Y. Feng, G. Ren, and X. Han. 2012. "Optimizing Feeding Composition and Carbon–Nitrogen Ratios for Improved Methane Yield During Anaerobic Co-Digestion of Dairy, Chicken Manure and Wheat Straw." *Bioresource Technology* 120: 78–83.

Wang, Z., M. Gerstein, and M. Snyder. 2009. "RNA-Seq: A Revolutionary Tool for Transcriptomics." *Nature Reviews Genetics* 10, no. 1: 57–63.

Willig, C. 2021. "Investigation of Genes Involved in Somatic Embryogenesis and Plant-Agrobacterium Interactions Through Transcriptional Profiling (Doctoral Dissertation, University of Missouri-Columbia)."

Wortmann, C. S. 2006. "Nitrogen Use Efficiency in Sorghum and Maize." *Field Crops Research* 96: 185–191.

Wu, X., H. Liu, W. Wang, et al. 2021. "OsNLP4 is Involved in Adaptation to Nitrogen Deficiency in Rice." *Plant Journal* 105, no. 5: 1301–1315. https://doi.org/10.1111/tpj.15131.

Xia, J., Y. Zhao, P. Burks, M. Pauly, and P. J. Brown. 2018. "A Sorghum NAC Gene Is Associated With Variation in Biomass Properties and Yield Potential." *Plant Direct* 2, no. 7: e00070.

Xu, G., X. Fan, and A. J. Miller. 2012. "Plant Nitrogen Assimilation and Use Efficiency." *Annual Review of Plant Biology* 63: 153–182.

Xu, Y., F. Yan, Y. Zong, et al. 2022. "Proteomic and Lipidomics Analyses of High Fatty Acid AhDGAT3 Transgenic Soybean Reveals the Key Lipase Gene Associated With the Lipid Internal Mechanism." *Genome* 65, no. 3: 153–164.

Yang, J., and M. Udvardi. 2018. "Senescence and Nitrogen Use Efficiency in Perennial Grasses for Forage and Biofuel Production." *Journal of Experimental Botany* 69, no. 4: 855–865.

Yang, W., J. Yoon, H. Choi, Y. Fan, R. Chen, and G. An. 2015. "Transcriptome Analysis of Nitrogen-Starvation-Responsive Genes in Rice." *BMC Plant Biology* 15, no. 1: 1–12.

Yao, X., J. Nie, R. Bai, and X. Sui. 2020. "Amino Acid Transporters in Plants: Identification and Function." *Plants* 9, no. 8: 972.

Yoshinaga, S., T. Takai, Y. Arai-Sanoh, T. Ishimaru, and M. Kondo. 2013. "Varietal Differences in Sink Production and Grain-Filling Ability in Recently Developed High-Yielding Rice (*Oryza sativa* L.) Varieties in Japan." *Field Crops Research* 150: 74–82.

Yu, J., G. Pressoir, W. H. Briggs, et al. 2006. "A Unified Mixed-Model Method for Association Mapping That Accounts for Multiple Levels of Relatedness." *Nature Genetics* 38, no. 2: 203–208. https://doi.org/10.1038/ng1702.

Zhang, D., W. Li, C. Xin, W. Tang, A. E. Eneji, and H. Dong. 2012. "Lint Yield and Nitrogen Use Efficiency of Field-Grown Cotton Vary With Soil Salinity and Nitrogen Application Rate." *Field Crops Research* 138: 63–70.

Zhang, Z., G. Chu, L. Liu, et al. 2013. "Mid-Season Nitrogen Application Strategies for Rice Varieties Differing in Panicle Size." *Field Crops Research* 150: 9–18.

Zhang, Z., W. Qiu, W. Liu, et al. 2021. "Genome-Wide Characterization of the Hyperaccumulator Sedum Alfredii F-Box Family Under Cadmium Stress." *Scientific Reports* 11, no. 1: 1–12.

Zhao, Q., L. Tong, A. Swami, and Y. Chen. 2007. "Decentralized Cognitive MAC for Opportunistic Spectrum Access in Ad Hoc Networks: A POMDP Framework." *IEEE Journal on Selected Areas in Communications* 25, no. 3: 589–600.

Zhao, Y., X. Zhong, G. Xu, et al. 2024. "The F-Box Protein OsFBX156 Positively Regulates Rice Defence Against the Blast Fungus Magnaporthe Oryzae by Mediating Ubiquitination-Dependent Degradation of OsHSP71. 1." *Molecular Plant Pathology* 25, no. 6: e13459.

Zhou, W., S. Song, S. S. K. Dossou, et al. 2022. "Genome-Wide Association Analysis and Transcriptome Reveal Novel Loci and a Candidate Regulatory Gene of Fatty Acid Biosynthesis in Sesame (*Sesamum indicum* L.)." *Plant Physiology and Biochemistry* 186: 220–231.

Zhu, J. K. 2016. "Abiotic Stress Signalling and Responses in Plants." *Cell* 167, no. 2: 313–324.

Supporting Information

Additional supporting information can be found online in the Supporting Information section. **Figure S1:** Homology of the GWAS and RNA Seq identified candidate genes with other cereal crops. **Figure S2:** fes370174-sup-0002-FigureS2.docx. **Figure S3:** fes370174-sup-0003-FigureS3.docx. **Table S1:** fes370174-sup-0004-TableS1.xlsx. **Table S2:** fes370174-sup-0005-TableS2.xlsx. **Table S3:** fes370174-sup-0006-TableS3.xlsx. **Table S4:** fes370174-sup-0007-TableS4.xlsx. **Table S5:** Putative candidate genes identified through GWAS and RNA sequencing and their homology across different cereal crops.